



# Hazard estimation of Kashmir Basin, NW Himalaya using probabilistic seismic hazard assessment

Maqbool Yousuf<sup>1</sup> · Kaiser Bukhari<sup>1</sup>

Received: 14 March 2020 / Accepted: 9 September 2020 / Published online: 20 September 2020  
© Institute of Geophysics, Polish Academy of Sciences & Polish Academy of Sciences 2020

## Abstract

This study presents hazard estimation of Kashmir Basin, NW Himalaya using regional ground motion relations, representing one of the most seismically active region in the Himalayan belt. Fault-level seismic recurrence parameters are determined from an updated earthquake catalogue spanning from 25 to 2018 AD for all possible seismic sources. The estimated hazard maps are presented for three ground motion parameters (PGA, short and long period spectral acceleration) for 50, 100, 500 and 2500 years return periods. Moreover, uniform hazard response spectrums and hazard curves are presented for all ten districts of the basin. The southern section of the basin consisting districts of Budgam, Shopian, Pulwama and Kulgam show higher hazard levels due to presence of numerous seismogenic structures in close vicinity. Our results highlight that the imposed seismic hazard in Kashmir basin is highly underestimated which need to be redressed by modifying the current provisional design standards.

**Keywords** Himalaya · Hazard estimation · PSHA · UHRS · Kashmir Basin

## Introduction

The Kashmir basin (KB) is situated in the NW portion of the Himalaya. The basin sits close to Indo-Eurasian plate boundary and within the reach of earthquakes from numerous tectonically active sources in and around the basin. The area has been hit by numerous destructive earthquakes documented in historical records, like notable events of 844, 1123, 1501, 1555, 1735, 1778, 1828, 1863, 1885, 1905 and 2005 which caused destructive effects on natural and built environment with estimated EMS intensity VII–VIII for most of these quakes (Yousuf et al. 2020). With high seismicity in this region, the excessive increase in the population has resulted in large exposure to the seismic vulnerability (Bukhari et al. 2018; Yousuf et al. 2018, 2020; Bilham 2019). The vulnerability of the present population can be significantly mitigated by providing awareness on disaster mitigation and preparedness. Hence, the need of the hour is to robustly and reasonably estimate the existing seismic hazard of KB.

The erstwhile seismic hazard studies in the India and particularly present studied region (Khattari et al. 1984; Bhatia et al. 1999; BIS 2002; Parvez et al. 2003; NDMA 2011; Nath and Thingbaijam 2012) specify that these hazard assessments were established on empirical relations developed for provinces with entirely different geological, seismotectonic settings. NDMA (2011), formulated new empirical relations (A classes) for Indian mainland and adjoining areas while considering the regional geological and seismotectonic setting of India. Nonetheless, without incorporating the local site effects these ground motion relations prove imprecise to region-specific seismic hazard assessment, due to incomplete consideration of seismic source data and recurrence parameters which were acquired from previous assessments (Kotha et al. 2016, 2017). Therefore, in present study, the established regional ground motion relations (GMPE) by NDMA (2011) are corroborated with existing and widespread NEHRP classes B and C site conditions to assess the existing level of seismic hazard in the KB.

In present study, the site-specific probabilistic seismic hazard analysis (PSHA) of KB (33° 30' N–34° 40' N and 73° 45' E–75° 35' E) was estimated using Cornell–McGuire approaches (Cornell 1968; McGuire 1976), Stochastic Seismological Model of Motazedian and Atkinson (2005), modified by Boore (2009) and applying the regional ground

✉ Maqbool Yousuf  
makyousuf@hotmail.com

<sup>1</sup> Department of Civil Engineering, National Institute of Technology, Srinagar, Jammu and Kashmir, India

motion relations (NDMA 2011). NDMA (2011) delineated 32 seismogenic zones in India among which 8 zones are found within a 500 km radius of the KB. 317 faults/seismogenic sources exist within these zones (GSI 2000), which represent possible seismic sources. By means of a simple empirical deaggregation technique (after Iyengar and Ghosh 2004; NDMA 2011), recurrence parameters were calculated for different seismic sources from an updated earthquake catalogue spanning from 25 to 2018 CE.

Hazard estimations for three ground motion parameters (i.e. peak ground acceleration (PGA), long period (1.0 s) and short period (0.2 s) spectral acceleration) are displayed as contour maps. The maps are presented for 50, 100, 500 and 2500 year return periods with 2 and 10% probability of exceedance in 50 years. Further, uniform hazard response spectrum (UHRS) along with hazard curves (HC) are presented for all ten districts.

## Geological and tectonic setting of Kashmir Basin (KB)

### General characteristics of KB

Kashmir basin or Kashmir Valley, a distinct geological entity, represents one of the two Meso-provinces (Jammu and Kashmir) of Jammu and Kashmir Union territory, India, divided by the gigantic Himalayan mountain ranges from one another. The valley extending between  $33^{\circ} 30' \text{ N}$ – $34^{\circ} 40' \text{ N}$  and  $73^{\circ} 45' \text{ E}$ – $75^{\circ} 35' \text{ E}$  with an aerial extent of  $6158 \text{ mi}^2$  ( $15,948 \text{ km}^2$ ) (Fig. 1). It portrays a northwest-southeast trending elongated oval shaped depression/basin,  $\sim 140 \text{ km}$  long and  $\sim 35$ – $40 \text{ km}$  wide, with Jhelum River draining it. The oval shaped KB is filled with thick deposits of Quaternary-Holocene sediments known as Karewas which are overlain by recent alluvium. The basin is confined within lofty mountain ranges, like by Pir Panjal Range on south, Kazinag Range on southwest, Saribal Range on the southeast and the Greater Himalayan range on the northern side. The basin has an average elevation of  $1620 \text{ m}$  ( $5314 \text{ ft.}$ ) amsl. The altitude varies from  $1088 \text{ m}$  (Jhelum gorge,

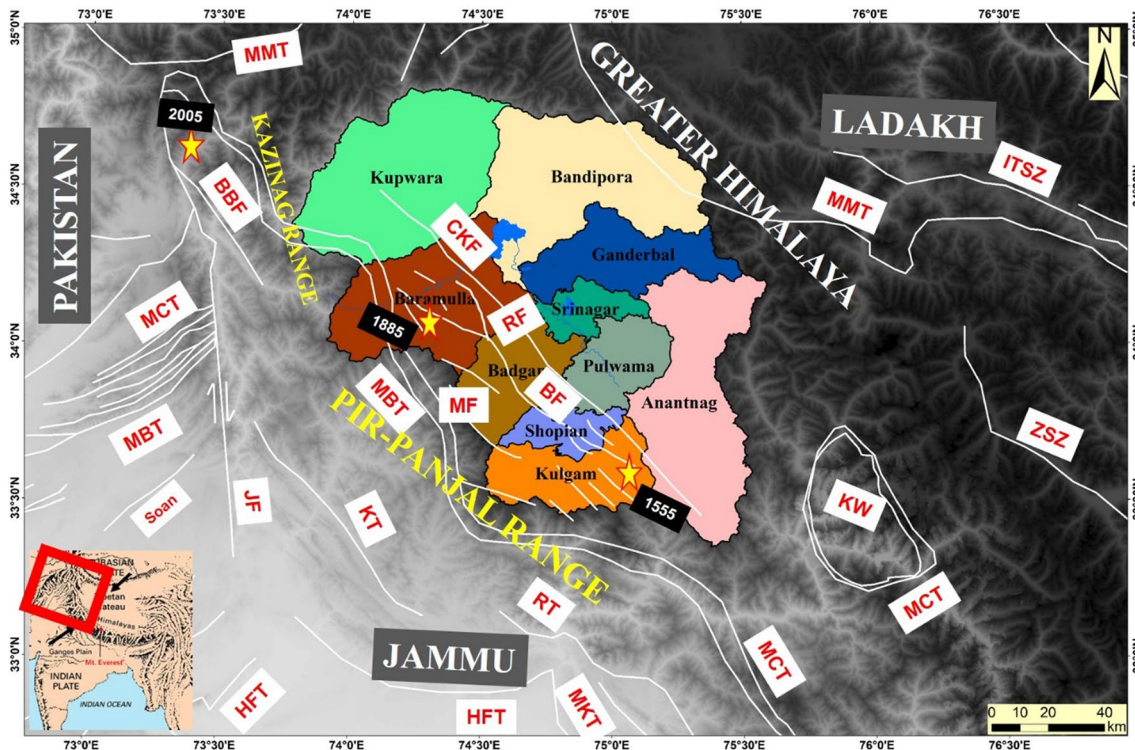


**Fig. 1** Structural and tectonic map of the Kashmir Valley and adjoining regions along with the administrative districts of the Kashmir Valley. The yellow stars show the possible location and timing of historical earthquakes (BBF Bagh Balakot Thrust; Balapur fault and associated structures, CKF Central Kashmir Basin Fault, ITSZ Indus-

Tsangpo Suture Zone, JF Jhelum Fault, KW Kishitwar Window, KT Kotli Thrust, MMT Main Mantle Thrust, MCT Main Central Thrust, MBT Main Boundary Thrust, MF Middlemiss Fault, MKT Mandli-Kishanpur Thrust, BF, RF Raithan Fault, RT Riasi Thrust, ZT Zaskar Shear Zone)

in Baramulla District) in the south in Pir Panjal range to 5458 metres (Machoi Peak, in Ganderbal District) on the northern side in the Greater Himalaya. The KB shares borders on southern side with Jammu, on the east with Ladakh and on north and northwest with Line of Control with Pakistan. Demarcated as Kashmir division in the UT of Jammu and Kashmir, it is divided into ten administrative districts: Anantnag, Baramulla, Bandipora, Budgam, Ganderbal, Kulgam, Kupwara, Pulwama, Shopian and Srinagar. Overall population of the valley is 6.883 million with the population density of  $450.06/\text{km}^2$  ( $1165.7/\text{mi}^2$ ) and population growth rate of +25.55% in past 10 years (5.482 million; 2001–2011) (Census 2001, 2011). The population is distributed unevenly with sparse in the hilly or high altitude regions while it is denser in the valley which is characteristic feature of population in hilly regions of India like Himalaya. The district Srinagar contains ~18% of the total valley's population within ~3% of the total area of KB, corresponding to the joint population of Pulwama, Kulgam, and Shopian districts. Therefore, this suggests that the seismic hazard and exposure in the Srinagar district is higher than other districts which in turn highlights the necessity to mitigate and prevent the future catastrophic consequences.

### Tectonic setting

The ongoing collision between the underthrusting Indian and overriding Eurasian plate has severely fractured the northern edge of Indian plate making it highly deformed and uplifted zone in the form of mighty Himalaya. The Himalaya has grown in height due to slip and uplift along different crustal size fractures/faults since the onset of collision. These large fault zones (*Main Frontal Thrust (MFT) where Siwalik ranges overthrust Indo-Gangetic plain; Main Boundary Thrust (MBT) where Lesser Himalaya overthrust the Siwalik ranges, and Main Central Thrust (MCT) where Greater Himalaya and Tibet overthrusting the Lesser Himalaya*), are seismically active with recurrent large magnitude earthquakes along these faults. The causative earthquakes are due to the continuous convergence between these two plates where Indian plate moves @ 40–45 mm/year with respect to Eurasian plate (DeMets et al. 1994), accumulating enormous strain in the Himalayan region, turning it to highly prone to earthquakes with disastrous future consequences, putting millions of people and civil infrastructure present within this belt (Bilham and Wallace 2005; Yousuf and Bukhari 2019, 2020; Yousuf et al. 2020). Historical earthquake data since 1897 suggest that at least 16 great earthquakes with  $M_w \geq 7.5$  have rocked this region (Mandal et al. 2000; Bilham 2004, 2019) with conspicuous damage to the life and built environment. According to Seismotectonic Atlas of India and its Environs (Dasgupta et al. 2000), more than 60% of area in India is highly prone/susceptible

to earthquakes due to the existence of large active seismogenic sources/faults both along the existing plate boundaries and within the continental interiors, which triggered large historical seismic events and have ability to trigger large-major seismic events in future as well. Wyss 2005; Bilham et al. 2001 predicted around 150,000 and 200,000 fatalities and very high economic loss due to future great Himalayan earthquakes. With 10% probability of exceedance, Dunbar et al. (2003) proposed around USD 350–650 million expected losses due to earthquakes in India for the next 50 years. The recent past earthquakes (since 1993) took a heavy toll of life and property (Table 1).

The Kashmir Valley in northwest Himalaya, has been hit by numerous earthquakes in recent past. Ten major earthquakes with magnitude  $> 7M_w$  has hit this region in last 1000 years (Iyengar et al. 1999; Ahmad et al. 2009; Bilham 2019; Yousuf et al. 2020). Some major earthquakes with appreciable historical record of its colossal damage are the 1555 Kashmir Earthquake ( $M_w$  7.4), 1885 Baramulla earthquake ( $M_w$  6.8), and 2005 Kashmir Earthquake ( $M_w$  7.6). These earthquakes triggered severe damages in this region and such seismic events highlight the hazard imposed by future seismicity.

According to McGuire–Cornell approach, the assessment of the apparent ground motion strength at a specific site depends on the comprehensive knowledge of the seismic sources along with their seismic activity within an effective distance from the site (i.e. source to site distance). The earthquake sources, within a radius of 500 km around the KB whose seismic activity can appreciably cause damage in the region, were demarcated from the Seismotectonic Atlas of India (GSI 2000). On the basis of presence of different seismic sources and resultant seismicity, NDMA (2011) classified the India into 32 seismogenic zones. Eight seismogenic zones out of these 32 zones are situated within 500 km radius of KB, and are taken into consideration during PSHA evaluation in present study. The seismogenic zones around the study area include (1) Western Himalaya (SZ-1), (2) Alta Togh and Karakoram (SZ-6), (3)

**Table 1** List of notable earthquakes with colossal damage to both life and economy since 1993 in India

Earthquake	Mag-nitude ( $M_w$ )	Loss of life	Economic loss
1993 Latur	6.2	11,000	USD 280 million–1.3 billion
1997 Jabalpur	5.8	38–56	USD 37–143 million
1999 Chamoli	6.6	103	USD 1.3 billion
2001 Bhuj	7.7	2,27,000	USD 4.6 billion
2005 Kashmir	7.6	> 1,00,000	USD 2.3 billion
2011 Sikkim	6.9	111	USD 22.3 billion

Sindh-Punjab (SZ-21), (4) Upper Punjab and West-Pakistan (SZ-22), (5) Kirthar-Sulaiman (SZ-23), (6) Chaman Fault (SZ-26), (7) Aravali-Bundelkhand (SZ-28), (8) Hindukush (SZ-30) zones (Fig. 2).

The Kashmir Valley completely falls within the Western Himalaya zone (SZ-1) which represents an active plate margin, characterized as highly deformed zone with several noticeable seismogenic structures. Figure 1 clearly shows presence of large-sized faults located near highly populated areas. The districts of Kulgam, Anantnag, Shopian, Pulwama and parts of Budgam lies very close to the active Balapur Fault (BF), even crossing across most populated towns and villages. The Jhelum Fault, a blind fault, runs parallel to Jhelum valley in EW direction of the basin traversing the districts of Anantnag, Pulwama, Srinagar and Bandipora. Kolbugh Fault causative of 1953  $M_w$  5.3, an active blind thrust, traverses in NW–SE direction across the Pulwama and Budgam districts. The Hayatpor-Watnu/Baramulla Lorrider Fault runs in NW–SE direction through the districts of Baramulla and Budgam. The MCT also referred as the Panjal thrust, traverses through the southern extremes of the basin across the districts of Baramulla and Budgam. South of MCT lies the Main Boundary Thrust also referred as Murree Thrust. Nearly 700 km long segmented Medlicott-Wadia Thrust (MWT) (Bagh-Balakot Fault (BBF), Kotli Thrust (KT), Raise Thrust (RT), Mandali-Kishanpur Thrust

(MKT), Bilaspur Thrust (BT), Palampur Thrust (PT) lies further south of MBT. On to the south nearly 100 km from KB lies the Himalayan Frontal Thrust (HFT), the present surficial expression of plate boundary basal decollement in the form southward moving anticlinal feature the Surian-Mastargh Anticline (SMA). To the north of Kashmir basin lies the Indus-Tsangpo Suture Zone (ITSZ), Main Mantle Thrust (MMT)/Great Counter Thrust (GCT), South Tibetan Detachment Zone (STD) and numerous small to large folds and faults.

Zone SZ-6 comprises the Altyn-Tagh fault system and left lateral, strike-slip Karakoram fault system. Zone SZ-21 comprises the seismic sources present in and around the Sindh-Punjab section. SZ-22 comprises the Upper Punjab and West-Pakistan fold-and-thrust belts which are imbrications/splays of east ward extending MCT, MBT and HFT. Zone SZ-23 is a large section comprising highly deformed geotectonic setup with high seismicity, comprising complex fold-and-thrust belt of Kirthar-Sulaiman mountain ranges. Zone SZ-26 contains 850 km long Chaman Fault, a left-lateral transform fault delimiting the Eurasian plate from the Indo-Australian plate. Zones SZ-28 comprises numerous seismogenic sources mostly blind thrust faults of Indo-Gangetic plains in West UP and East Punjab including Delhi. Zone SZ-30 consists of deep focal earthquake zone around Hindukush region. Three hundred and

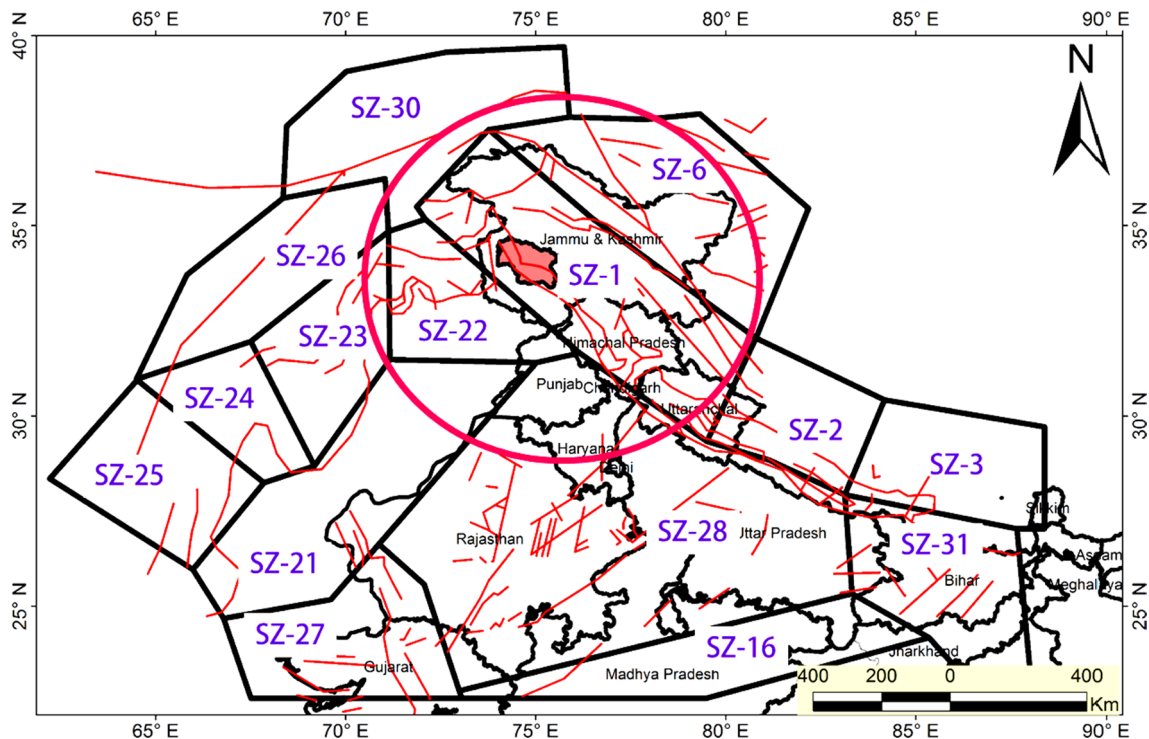


**Fig. 2** Different seismogenic zones as well as source/faults present around Kashmir Basin. A total of 317 fault are delineated within eight considered seismogenic zones (SZ-1, SZ-6, SZ-21, SZ-22,

SZ-23, SZ-26, SZ-28, SZ-30) around the study region (highlighted in red) taken as likely seismic sources. Red circle defines 500 km buffer zone around the study region



seventeen seismogenic sources/faults present within these 8 source zones are considered in this study along with their seismicity (Figs. 2, 3). Although, certain past earthquakes witnessed in this region can be linked with known seismogenic sources, while some cannot be associated to particular seismogenic sources due to lack of substantial data about location, size and timing of the earthquake (Fig. 3a). In PSHA framework, earthquake parameters of the different seismogenic sources are selected from the Gutenberg–Richter (G–R) recurrence relationship obtained from the updated earthquake catalogue of the study area.

## Determined earthquake catalogue

In present study, an updated earthquake catalogue for these source zones has been used consisting the instrumentally recorded events of magnitude  $M_w \geq 4$  for the period 1970–2018 A.D obtained from different databases [United States Geological Survey (USGS), International Seismological Centre (ISC), Indian Meteorological Department (IMD), Pakistan Meteorological Department (PMD)], etc. The additional historical events (Quittmeyer and Jacob 1979; Iyengar et al. 1999; Ambraseys 2000; Ambraseys and Jackson 2003; Ambraseys and Douglas 2004; Ahmad et al. 2009; Bilham and Bali 2013; Ahmad and Shafi 2014; Bilham 2019) were homogenized and converted to  $M_w$  magnitude scale following universal magnitude conversion scale (Scordilis 2006) magnitude conversion methodology.

$$M_s - M_w$$

$$M_w = 0.67M_s + 2.07, \quad \text{for } (3.0 \leq M_s \leq 6.1) \quad (1)$$

$$M_w = 0.99M_s + 0.08, \quad \text{for } (6.2 \leq M_s \leq 8.2) \quad (2)$$

$$m_b - M_w$$

$$M_w = 0.85m_b + 1.03, \quad \text{for } (3.5 \leq m_b \leq 6.2) \quad (3)$$

In PSHA framework, seismic events are considered to be Poissonian, where the foreshocks and aftershocks events are distinguished from main shock and subsequently excluded. In this study, we followed Gardner and Knopoff (1974) and Uhrhammer (1986) declustering approach which distinguishes the foreshocks and aftershocks from main shocks from seismic clusters on the basis of temporal and spatial distribution of these seismic events. Historical as well as instrumentally recorded data from 25 to 2018 CE, within considered eight seismic source zones show 6405 individual events or main shocks. These include  $4 \leq M_w \leq 4.4$  (3018 events),  $4.5 \leq M_w \leq 4.9$  (2023 events),  $5 \leq M_w \leq 5.4$  (860

events),  $5.5 \leq M_w \leq 5.9$  (280 events), and  $6 \leq M_w \leq 6.4$  (142 events),  $6.5 \leq M_w \leq 6.9$  (51 events)  $7 \leq M_w \leq 7.9$  (25 events), and  $> 8M_w$  (6 events) (Fig. 3b). The updated earthquake catalogue shows spatial occurrence of high frequency of low magnitude events and low frequency of high magnitude events.

The sequential distribution of the seismic events (Fig. 4) reveals that the low magnitude seismic events data are available for the last few decades only (1972 onwards) while the large magnitude seismic events occur at an uneven rate with large spatial and temporal variation. Hence, it becomes essential to establish completeness interval of considered earthquake catalogue for all applied magnitude ranges in order to determine their recurrence parameters. In order to overcome this issue, we followed Stepp (1972) completeness test approach to determine the incomplete (or historic) and complete part of the considered earthquake catalogue. This method considers backward projection of the occurrence rates of different observed seismic events and their respective magnitudes for different time periods from the last catalogue date (2018 in present study). To analyse the completeness of earthquake events, all the considered events are grouped in different magnitude intervals. Each magnitude range is represented as point process in time. The variance of the sample mean is inversely proportional to the number of observations in the magnitude range (Stepp 1972). To estimate the variance, the earthquake events modelled as Poisson distribution. If  $x_1, x_2, x_3 \dots x_n$  are the number of events per year in a magnitude range, then the mean rate for this sample is  $x = \left(\frac{1}{n}\right) \sum_{i=1}^n X_i$ , where  $n$  is the number of unit time intervals. The variance is given by  $\sigma_x^2 = \frac{x}{T}$ , where  $T$  is the duration of the sample. If  $\chi$  was to be constant,  $\sigma_\chi$  would vary as  $1/\sqrt{T}$ . Following Stepp (1972) the standard deviation of the mean rate as a function of sample length are plotted along with nearly tangent lines with slope  $1/\sqrt{T}$ . The deviation of standard deviation of the estimate of the mean from the tangent line indicates the length up to which a particular magnitude range may be taken to be complete. As long as the data are complete, the standard deviation will be proportional to  $1/\sqrt{T}$ . The determined complete and incomplete part of the catalogue (Figs. 4, 5) show that spatial distribution of events and completeness of magnitude ranges vary considerable with time which is due to non-availability of the data.

The updated catalogue shows varied rate of completeness for different magnitude scales with wide-ranged temporal distribution. It was observed that for  $4 \leq M_w \leq 4.4$  [completeness period of 37 years (1981–2018)],  $4.5 \leq M_w \leq 4.9$  [completeness period 48 years (1970–2018)],  $5 \leq M_w \leq 5.4$  [completeness period 48 years (1970–2018)],  $5.5 \leq M_w \leq 5.9$  [completeness period 58 years (1960–2018)],  $6 \leq M_w \leq 6.4$  [completeness period 113 years (1905–2018)],

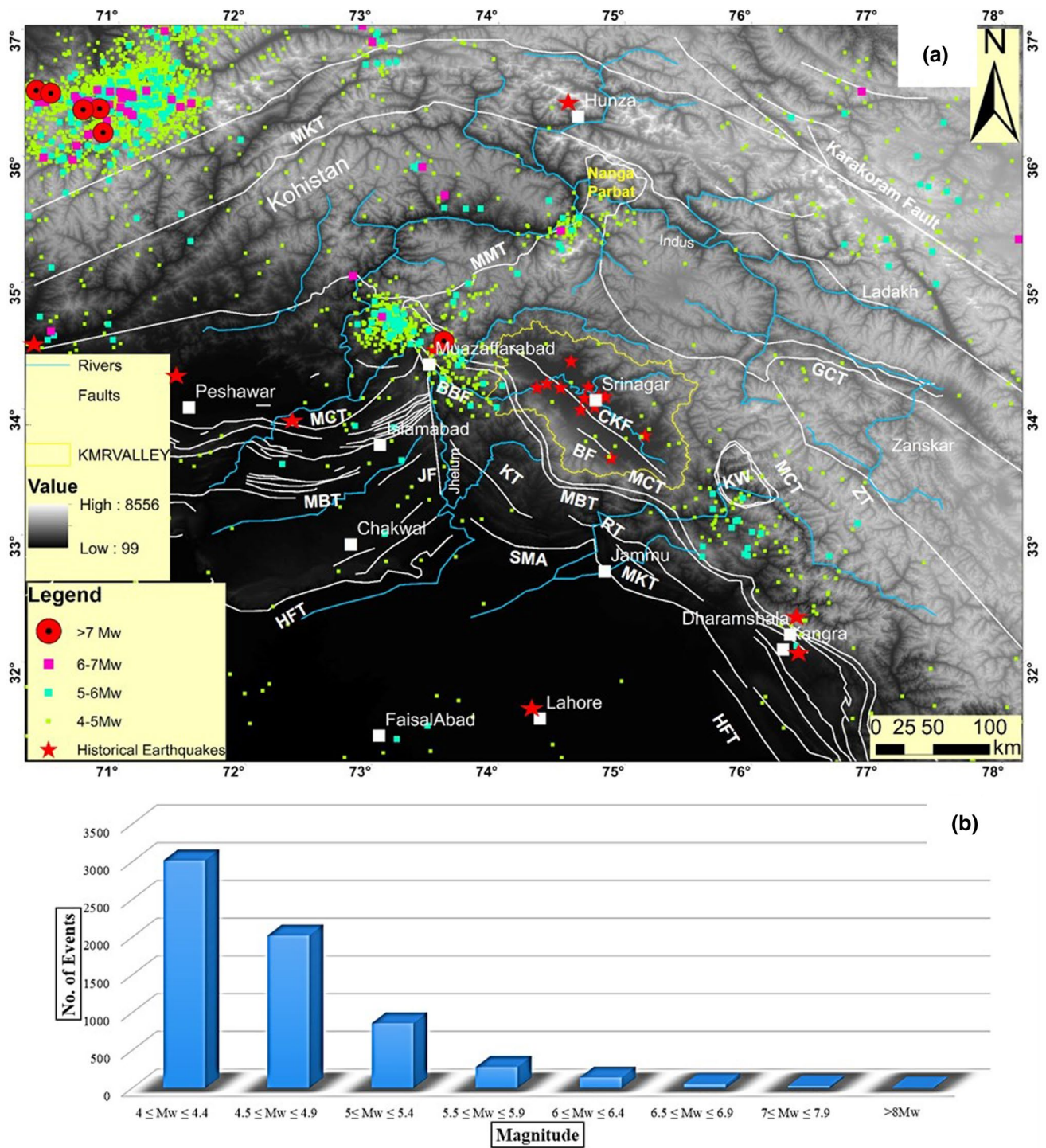


**Fig. 3** **a** The epicentral location of instrumental recorded earthquakes ( $>4M_w$ ) and historical great earthquakes of magnitude  $M_w \geq 6.8$  (red stars). **b** Graphical representation of number of seismic events with respect to their magnitude

$6.5 \leq M_w \leq 6.9$  [completeness period 133 years (1885–2018)], and  $7 \leq M_w \leq 7.9$  [completeness period 463 years (1555–2018)].

**Ground motion prediction equations (GMPE)**

Most of the previous seismic hazard assessments carried out around Kashmir basin lack some basic features. (I) The previous studies did not consider the regional tectonic and

structural setting along with site characterization during hazard estimation which led to underestimation of the imposed hazard. (II) The derivation of hazard curves at regional level without considering the local geological, geotechnical and seismotectonic scenarios (III) the GMPE employed for hazard assessment were derived for regions with totally different geological, geotechnical and seismotectonic setup. This framework takes into account all known seismic sources/faults based on the historical seismicity, tectonic features and geology. Such seismic sources which have produced seismic events in the past and are capable of producing future seismic events have been extensively studied by NDMA (2011) before their consideration as seismogenic source model. Hence in present study these gaps were considered by incorporation GMPE specifically derived for this region by NDMA (2011).

## Recurrence parameters

In present study, we followed empirical Gutenberg–Richter (GR) recurrence relationship to determine the recurrence interval and seismicity rate of the existing seismic sources/faults present within the considered eight seismogenic zones. The GR relation provides information about the capability as well as frequency of particular source/fault to trigger a given magnitude. It determines mean annual rate of exceedance  $\lambda_M$  of an earthquake of magnitude  $M$ , triggered by the source in a time period  $T$  and is expressed as

$$\log 10(\lambda_M) = a - bM \quad (4)$$

$a$  = logarithmic seismic level in terms of mean annual value,  $M$  = minimum considerable magnitude produced by the fault,  $b$  = frequency and potential of the fault to trigger earthquakes of particular magnitude.

As  $M_w < 4$  produce negligible structural damage and are not important from design perspective, we omitted all earthquakes with magnitude  $< 4M_w$  which provide  $M_w \geq 4$ .

To evaluate the different GR recurrence parameters ( $a$ ,  $b$ , and  $M_{\max}$ ), comprehensive evidence of seismicity of all the distinct faults is essential, however, such evidence are rare and almost not available for most of the sources/faults. Same scenario exists in this region with poor information about the recurrence rates of different faults. To overcome this issue, we first determined these parameters at zonal level for all eight considered seismic zones and subsequently deaggregated and assigned these parameters to each fault present within these zones following Kijko and Graham (1998) and Kijko (2004) approach which links the prehistoric or paleoseismic, historic and instrumental seismicity data to acquire the seismicity parameters required for PSHA analysis.

The  $a$  and  $b$  values estimated from the maximum likelihood method of Kijko and Graham (1998) and Kijko (2004). The parameters ( $a$ ,  $b$ ) values describe the seismic pattern of any area. Higher  $a$  value suggests higher seismicity of any region. “High  $b$ ” value indicates low occurrence rate of large magnitude earthquake, while as “low  $b$ ” value indicates high occurrence rate of large magnitude earthquakes. In present study the  $b$  value ranges from  $0.67 < b < 0.95$ . The uncertainty in the estimated  $b$  values lies in between 0.02 and 0.06. Since earthquakes occur frequently in Himalaya the catalogues contain complete information about the both small and damaging earthquakes, and hence, the uncertainty in the estimated parameters is low.

Knopoff and Kagan (1977) proposed that an upper bound for magnitude ( $M_{\max}$ ) must be established in the Gutenberg–Richter frequency magnitude. Hence in present study following Wells and Coppersmith (1994) approach, the maximum seismic potential  $M_{\max}$  of all the faults is considered to be the largest seismic event plus 0.5 units (uncertainty value) witnessed in the parental seismic zone assuming that all sources are capable of triggering such large events in future. However, uncertainty and incompleteness associated with earthquake catalogue exists which need to be ascertained for complete as well as incomplete part. Hence 0.5 for incomplete part and 0.3 for complete part are considered as magnitude uncertainty values (after NDMA 2011).

The determined GR recurrence parameters and the existing seismic source/faults in considered seismogenic zones are shown in Table 2. Most of these seismic source/faults possess a  $M_{\max}$  potential  $\geq 7M_w$ . Three zones among eight considered zones exhibit  $N_{(4)} > 2$  indicating potential to generate two seismic events of  $M_w \geq 4$ /year. The Western Himalaya zone (SZ-1), encompassing Kashmir basin, has witnessed highest seismic events due to presence of numerous active seismic sources in this zone. This suggests that high seismic rate and near site source seismic sources can trigger frequent as well as large magnitude earthquakes in close vicinity around Kashmir basin.

## Determination of fault-level recurrence parameters

The uneven nature of seismicity of different faults in these seismic zones exist, and hence, fault-level recurrences provide substantial data for seismic hazard analysis. Secondly, large uncertainty exists in the present earthquake catalogue along with very less data available about the slip rate and seismic activity for most of the faults present within these seismogenic zones. Iyengar and Ghosh (2004) provided an empirical relation to determine the recurrence rate at fault level. This relation considers zonal seismicity assessed from  $a$  value relating them to all faults. The fault slip rate as well as seismic activity assigned to each fault provides assumptive  $a$  value. In present study, the zonal seismicity



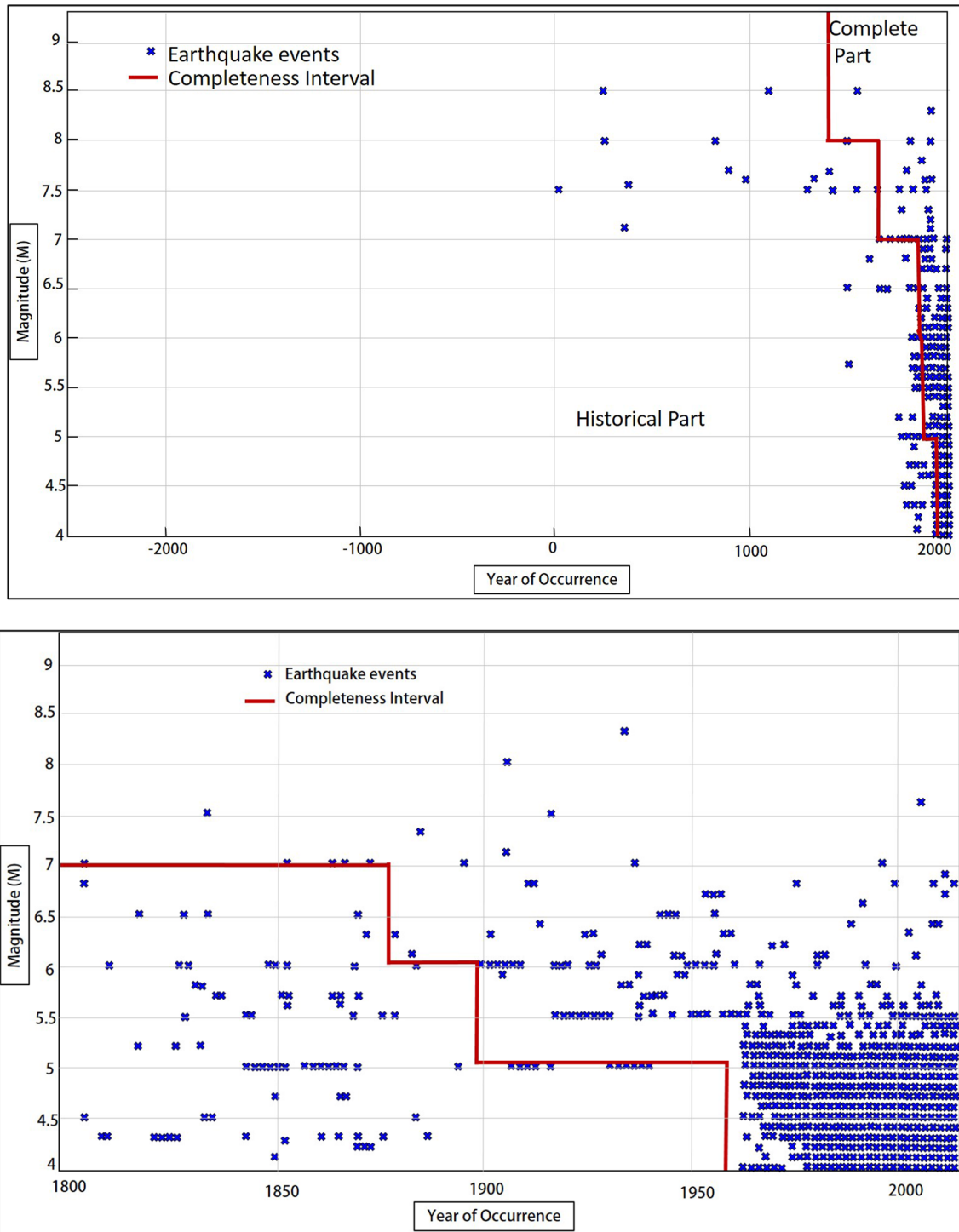


**Fig. 4** Sequential distribution of the earthquake events witnessed within the eight considered seismogenic zones (from 25 up to 2018 A.D.). The completeness interval attained by Stepp (1972) method is also showed by the red solid line

is correlated to nearby fault considering distance to nearby fault. The earthquakes are assigned to a particular fault which lies very close to the epicentre of the witnessed earthquake. Accordingly in present study, for any considered fault (*i*), the zonal *a* value is attributed to it equalled by a factor

ratio considering its characteristic (length and seismic activity of that fault). Accordingly, *a<sub>i</sub>* value of specific (*i*) fault is

$$a_i = N_i(m_o) = 0.5 \left( \frac{L_i}{L_z} + \frac{n_i}{N_z} \right) N(m_0) \tag{5}$$



**Fig. 5** Completeness test for earthquake data using Stepp (1972) method. Straight lines indicate the theoretical slope of complete data range

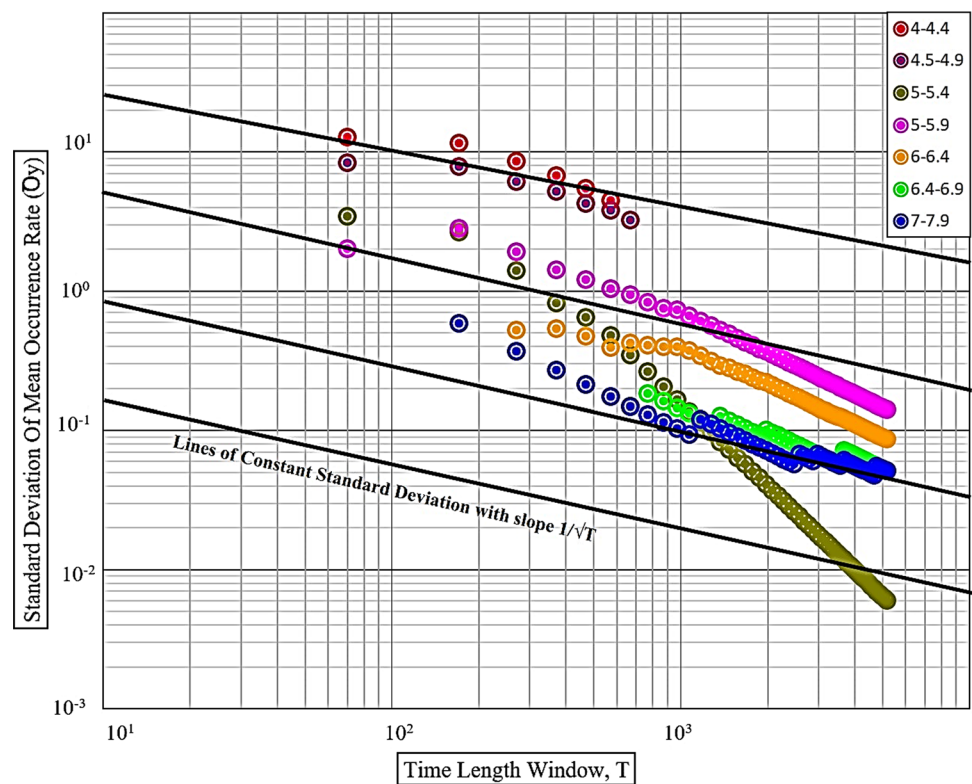


**Table 2** Observed seismic parameters for the eight seismogenic zones around Kashmir Basin

Source no.	Zones	<i>B</i> value	<i>N</i> (4)	Max. potential magnitude <i>M</i> <sub>max</sub>	Number of faults
SZ1	Western Himalaya	0.88 ± 0.02	5.73	8.8 ± 0.03	97
SZ6	Altya-Tegh and Karakoram	0.91 ± 0.03	7.10	7.3 ± 0.36	31
SZ21	Sindh-Punjab	0.77 ± 0.06	0.60	8.0 ± 0.17	11
SZ22	Upper Punjab and west-Pakistan	1.01 ± 0.05	1.68	7.8 ± 0.28	27
SZ23	Chaman Fault	0.74 ± 0.05	5.22	7.8 ± 0.13	13
SZ26	Kirthar-Sulaiman	0.84 ± 0.04	5.03	7.3 ± 0.11	43
SZ28	Aravali-Bundelkhand	0.81 ± 0.06	1.16	7.0 ± 0.31	68
SZ30	Hindu Kush	0.93 ± 0.01	83.54	8.0 ± 0.23	27

The fault length ratio equals to ratio of specific (*i*), fault length (*L<sub>i</sub>*) to the total zonal fault lengths ( $L_z = \sum_{i=1}^{N_s} L_i$ ). The fault activity ratio is the ratio of the event occurrences at the fault *n<sub>i</sub>* to total events in the zone *N<sub>z</sub>*. The total number of faults in specific zone is *N<sub>s</sub>* and *N*(*m*<sub>0</sub>) is seismic events with magnitude > 4 within a zone triggered from all the faults per year.

We assigned zonal *b* value to all seismic sources/faults and each fault has same *b* value due to large uncertainties regarding seismic parameters (magnitude, seismic potential and slip rate) of these faults. Similarly, following Wells and

Coppersmith (1994) approach, the maximum seismic potential *M*<sub>max</sub> of all the faults is considered to be the largest seismic event plus 0.5 units (uncertainty value) witnessed in the parental seismic zone assuming that all sources are capable to trigger such large events in future. Therefore, for all the 317 existing faults within eight seismogenic zones, the fault-level recurrence parameters were estimated following the Iyengar and Ghosh (2004) procedure (Fig. 6). While carrying out the PSHA framework, the estimated parameters for all individual seismic source/faults determine their seismic rate.

## Structure of probabilistic seismic hazard analysis (PSHA)

The estimation of the level of ground shaking, that has an effect on design life of any structure, in a deterministic manner, can be unreliable due to the various uncertainties involved in the source and site characteristics. To overcome this issue, Cornell (1968) proposed PSHA procedure to assess the level of earthquake hazard (as a function of ground shaking intensity) imposed at a specific site by considering the uncertainties produced by causative seismic sources/faults, their seismic activity, seismic wave propagating direction along with inherent properties of propagating path material and distance from causative source to specific site. The point source model in Cornell (1968) approach had some limitations, which Der Kiureghian and Ang (1977), updated this method by incorporating finite source model to characterise seismic sources along with their associated uncertainties. The uncertainties are generally categorized into aleatory and epistemic uncertainties acting as core design in the PSHA framework. In this method, the aleatory uncertainty is determined by using probability distributions of the source to site distance, magnitude and the ground motion relations. As the uncertainties decrease, the PSHA gets more validated once more seismic data (seismic and slip rate of sources) become accessible.

The procedure of PSHA carried out for present study is extensively discussed in the previous PSHA studies (Kramer 1996; NDMA 2011). Therefore in present study, the seismic hazard assessments are modified by presenting a notion that earthquakes triggered by a specific source are individual main shocks and therefore supposed to be Poissonian in nature. It makes things easier to estimate probability of exceedance for observed ground shaking within a given time ( $T$  in years).

$$P(Y > y^* \text{ in } T \text{ years}) = 1 - e^{-\mu_y^* T} \quad (6)$$

where  $\mu_y^*$  = mean annual rate of exceedance of the ground shaking intensity level  $y^*$  (and its reciprocal is the average return period of the earthquake ( $T_r$ ) able of generating  $y^*$ ).

All the source faults inside 500 km bufferzone around Kashmir basin considered as potential sources following the international standards (USNRC 1997) to evaluate the level of seismic hazard imposed at a particular location/site within the study area. Fault-level recurrence parameters of all possible sources are considered in this study for seismic hazard estimation.

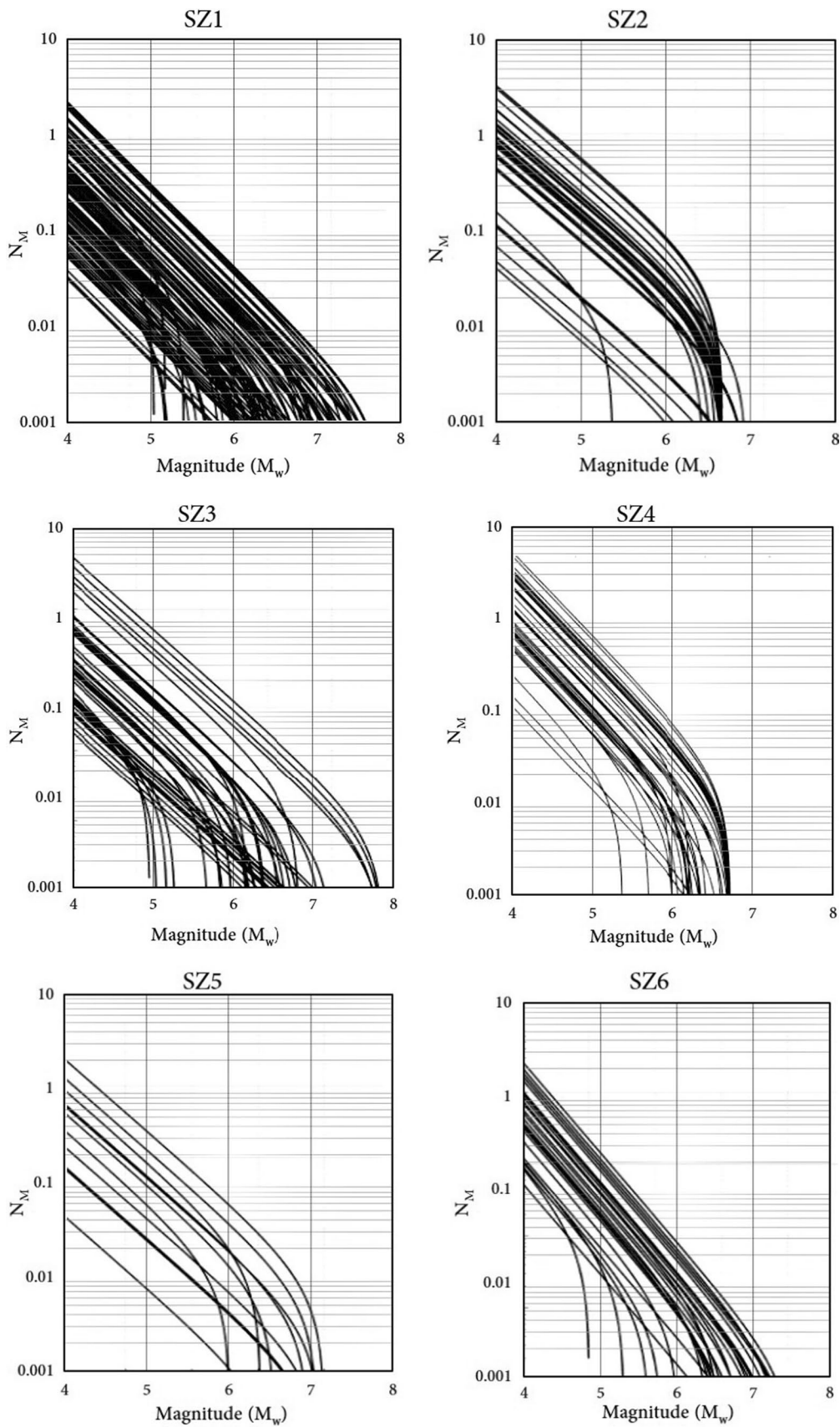
## Hazard estimation of Kashmir Basin

The probabilistic seismic hazard assessment of the KB (33° 30' N–34° 40' N and 73° 45' E–75° 35' E) is estimated at 0.1° grid interval in this study. Hazard maps are presented

**Fig. 6** Magnitude-frequency relations for all the seismic sources in the Eight seismogenic Zones (after Muthuganeisan and Raghukanth 2016 and present study)

in this study for three ground shaking intensity parameters, viz., peak ground acceleration (PGA), short period ( $S_a$ , 0.2 s) and long period ( $S_a$ , 1.0 s) spectral acceleration. Hazard maps showing level of seismic hazard are presented as iso-acceleration maps for 50, 100, 500 and 2500 year return period. These hazard maps were developed considering boundary between NEHRP classes B and C (rock site,  $V_s = 760$  m/s) as reference site condition. Moreover, seismic hazard curves for the 10 district-headquarters of Kashmir representing PGA values are also presented (Fig. 7). Uniform hazard response spectrum (UHRS)/design response spectra (Fig. 8) have been constructed at 5% damping for hard rock site conditions, from developed hazard maps for all districts, following IBC (2009) methodology.

The estimated PGA values in present study are in the ranges of 0.09–0.24 g, 0.16–0.44 g, 0.25–0.55 g and 0.37–0.72 g for of 50, 100, 500, 2500 years return period, respectively, with 2 and 10% probability of exceedance in 50 years (Fig. 9a–d). As expected, results show that the southern portion of the basin possess highest hazard which include districts of Shopian, Kulgam, Budgam, Baramulla, parts of Pulwama and Anantnag. This region has witnessed large number of damaging earthquakes. The high hazard can also be justified by the close proximity of seismic sources along the Pir Panjal front of the basin (e.g. Balapur Fault, Baramulla Lorridor Fault, Raithan Fault, Chanapor Fault, Hayatpor-Watnu Fault, Mawar Fault and associated structures; Fig. 1) (Yousuf et al. 2020). The highest PGA values observed are 0.24 g, 0.44 g 0.55 g and 0.72 g for 50, 100, 500 and 2500 year return period, respectively. These high PGA values are observed around and along the strike of Balapur Fault (active fault traversing the southern margin of basin mostly through Budgam, Shopian and Pulwama districts). Other areas of high hazard are located in the peripheries of Anantnag, Baramulla, Kulgam, parts of Kupwara and northern Ganderbal. The northern portion including Kupwara and Baramulla have been colossally damaged by 1885 ( $6.8M_w$ ) and 2005 ( $7.8M_w$ ) earthquakes and are also traversed by numerous active faults (Baramulla Lorridor Fault (Ahmad et al. 2014; Shah 2014), Hayatpor-Watnu Fault (Ahmad et al. 2015), Mawar Fault and associated structures (Shah and Malik 2017; Wani et al. 2019). The 1555 ( $7.4M_w$ ) earthquake caused severe damage mostly in the southern portion (Anantnag, Shopian, Kulgam, parts of Pulwama), although the causative fault is still unknown. The southern side is truncated by Balapur fault, nearly 110 km long, with substantial quaternary displacement (Madden et al. 2010, 2011), possess capability to generate large



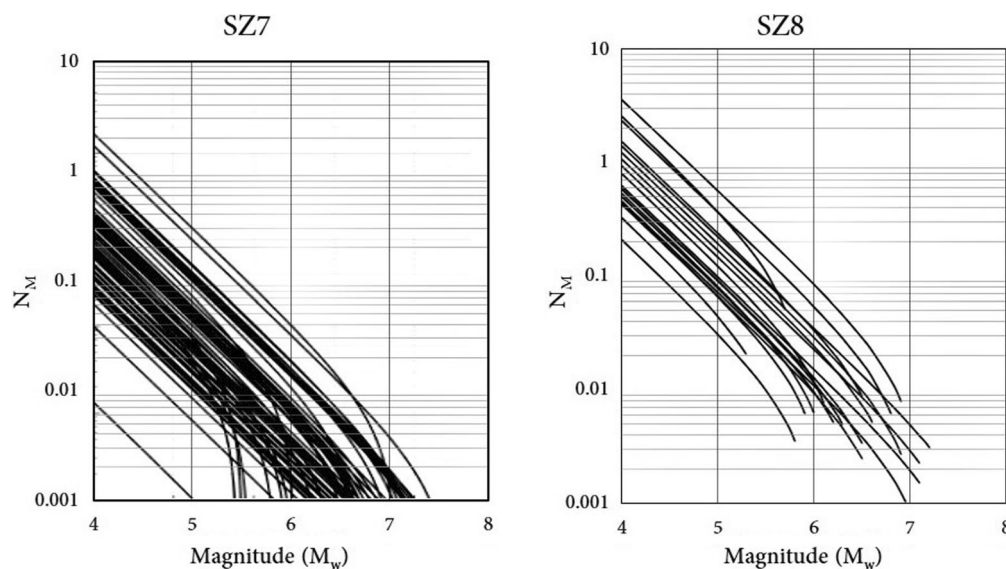


Fig. 6 (continued)

earthquakes ( $> 7M_w$ ) based fault length and seismotectonic setting (Ahmad et al. 2015).

Moreover, it is clear from hazard maps, that with increasing return periods hazard concentration increases to large areas as well as PGA values increase substantially. While as with low return periods the hazard is concentrated to smaller area. This can be validated by large stress accumulation in this region over time. The present geodetic results show nearly  $11 \pm 1$  mm/year (Schiffman et al. 2013) to  $17 \pm 2$  mm/year (Kundu et al. 2014) convergence rate, accumulating nearly 1 m slip potential per year in this region (Bilham 2019). Hence, more the gap between successive large earthquakes, high magnitude earthquakes can be expected for longer return periods ( $> 8M_w$ ). With availability of large seismic energy, the high PGA values can be expected with longer return periods.

Local site effects play a crucial part in seismic hazard estimation of any region. Most of the previous seismic hazard assessments carried out around Kashmir basin lack some basic features. (I) The previous studies did not consider the regional tectonic and structural setting along with site characterization during hazard estimation which led to underestimation of the hazard, (II) the GMPE employed for hazard assessment were derived for regions with totally different geological, geotechnical and seismotectonic setup. Hence in present study these gaps were considered by incorporation GMPE specifically derived for this region by NDMA (2011).

The earliest hazard assessment was carried out by Khattri et al. (1984), using attenuation curves of Algermissen and Perkins (1976), which are valid for the Eastern United States and proposed PGA values 0.4–0.7 g in Himalayan region.

Bhatia et al. (1999) used the attenuation relation defined by Joyner and Boore (1981) for California and the Western United States for whole Indian landmass and proposed PGA values 0.25–0.30 g in Himalayan region. Parvez et al. (2003) using deterministic seismic hazard assessment (DSHA) suggested 0.3–0.6 g for the Himalayan region. Mahajan et al. (2010), used attenuation relation Abrahamson and Litehiser (1989) and Peng et al. (1985) and estimated maximum PGA as high as 0.75 g for Himalayan region. As per the national seismic hazard map of India (BIS 2002), Kashmir basin lies in Zone-V, which corresponds to the peak ground acceleration (PGA) of 0.4 g. PGA values (0.05–0.12 g) estimated by NDMA (2011) for class A sites, are much lower than present investigation. Nath and Thingbaijam (2012) used different the attenuation relations for whole Indian landmass and proposed PGA value of 0.33 g for Kashmir basin.

Most of these studies ignored local site condition as well as fault-level seismicity, leading to underestimation of seismic hazard. In order to assess the seismic hazard at local level these studies conducted at much larger scale are not sufficient, so the results of these studies cannot be applied in the development of region-specific standard building code to design the earthquake resistant structures, land-use planning, hazard management, risk assessments and mitigation. The near source faults in this region have capability to produce very high PGA ( $> 1$  g), as have been observed during 2005 Kashmir earthquake (Raghukanth 2008). Therefore, in present study, by considering fault-level seismicity, the estimated hazard maps are more realistic and reliable.

Although, for design perspective of simple regular structures, PGA values are sufficient to determine their behaviour during seismic loading. However, tall and irregular



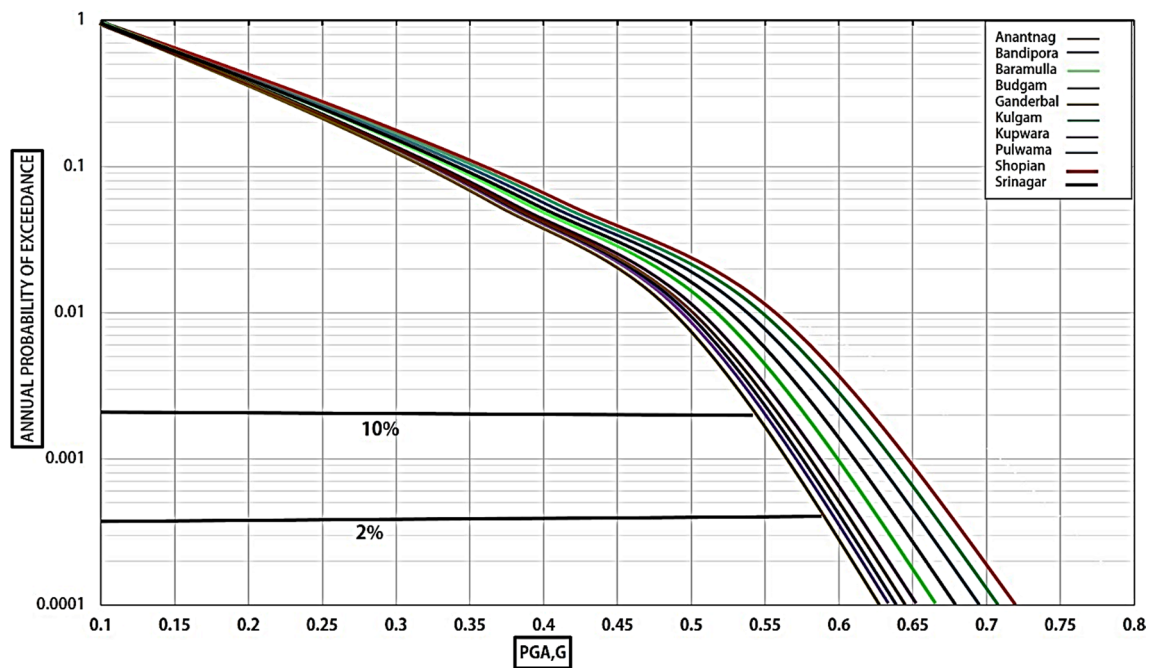


**Fig. 7** The seismic hazard curve for predicted peak ground acceleration (PGA) in g for ten districts of Kashmir basin, showing 2% and 10% probability in 50 years

structures display complex behaviour during seismic loading, hence dynamic analysis is required to evaluate their seismic behaviour (IS: 1893 2002, 2007; IBC 2009). Hence, in present study, for dynamic analysis of tall or irregular structures spectral accelerations maps are provided for both short period  $S_a$  (0.2 s) (Fig. 10a–d) and long period  $S_a$  (1.0 s) (Fig. 11a–d) for 50, 100, 500, and 2500 year return periods.

In present study, we observed that for 50-year recurrence period highest spectral acceleration ranges from 0.29 g for 0.2 s and 0.34 g for 1.0 s, respectively. Since for magnitude 4.5–5 $M_w$  events, return periods are very low and are frequent in this region, they contribute highest hazard if triggered within 5–10 km from the specific sites. Though, such earthquakes can produce high PGA values close to epicentre, but due to their short duration and low energy content their potential for extensive destruction is limited. However, large magnitudes at larger distances do contribute to higher hazard. For 100 years (highest spectral acceleration 0.53 g for 0.2 s and 0.62 g for 1.0 s), magnitude 5.0–6.0 $M_w$  events govern the hazard level within an epicentral distance of 10–15 km. At 500 and 2500 years (highest spectral accelerations of 0.68 g for 0.2 s and 0.73 g for 1.0 s and 0.73 g for 0.2 s and 0.87 g for 1.0 s, respectively), we observed that magnitude 6.5–7.5 $M_w$  events at located within a 15–20 km radius contribute most hazard like 2005 Kashmir earthquake. Nonetheless, considering such high ground shaking levels, 5 $M_w$

earthquakes or lesser (> 4.5 $M_w$ ) significantly influence the hazard level, however, the source to site distance controls the level of ground at the site. In Himalayan region the occurrence of shallow focal earthquakes greatly enhances the level of hazard. In Kashmir basin, most earthquake are shallow with focal depth between 5 and 40 km, which suggest higher hazard levels by even small magnitude earthquakes. Since the return period of large magnitude earthquakes (> 7.6 $M_w$ ) in Kashmir is more than 500 years, therefore for 500 and 2500 year return period large magnitude earthquakes (> 7.6 $M_w$ ) contribute the maximum hazard.

Due to complex geologic and tectonic setup of Kashmir basin, earthquakes triggered by near or far sources can substantially affect the level the seismic hazard. The thickness of the sediment covers above the bedrock and lateral variations in sediment thickness cause surface-wave amplification and greatly influence the degree of ground shaking during an earthquake. Basins filled with thick sediment layers show significant surface-wave amplification during earthquakes e.g. Mexico City during 7.6  $M_w$  Michoacan earthquake of 1911 (Sing and Ordaz 1993; Cárdenas and Chávez-García 2003) and San Francisco during the 6.9  $M_w$  Loma Prieta earthquake of 1989 (Stidham et al. 1999). Kashmir basin filled with ~1300 m thick Karewa deposits overlain by recent alluvial deposits. These thick sedimentary piles significantly affect seismic wave amplitude and level of shaking during an earthquake

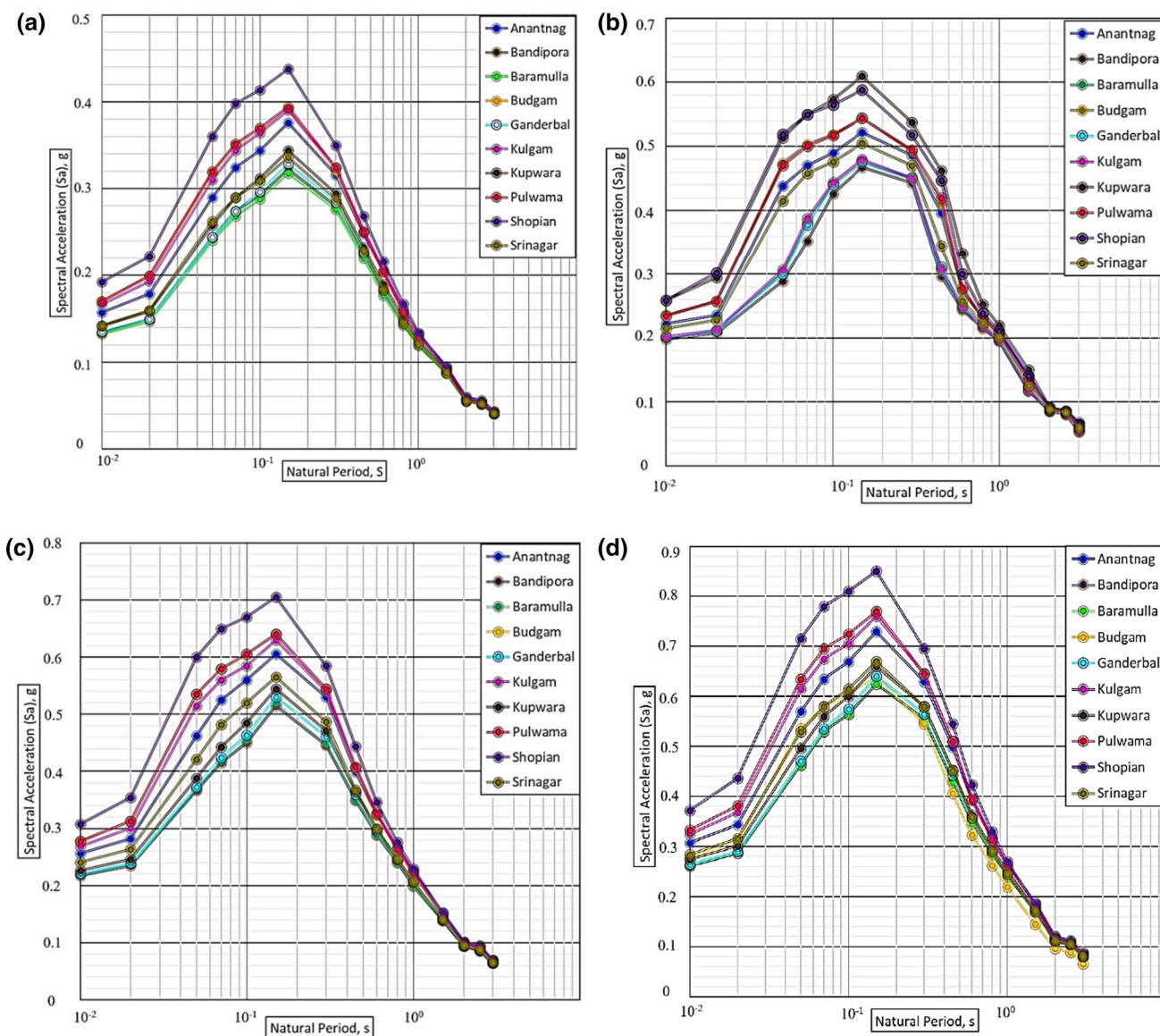
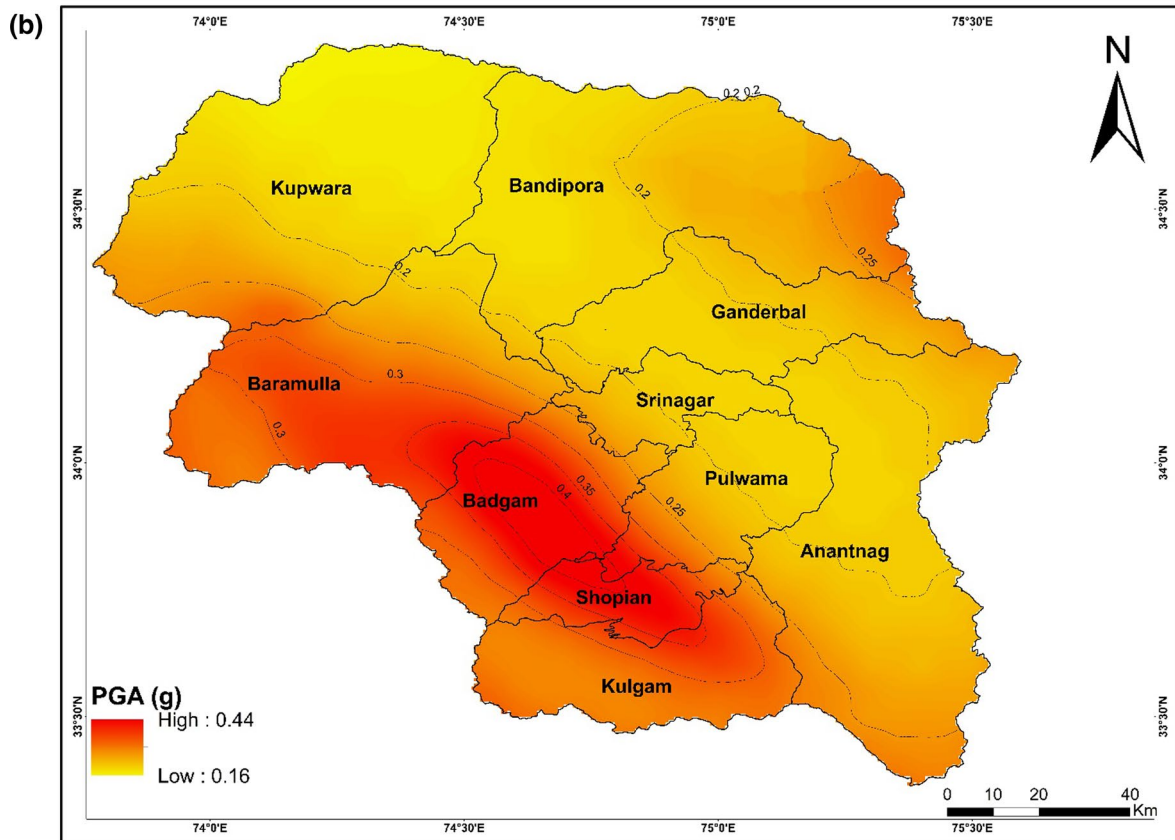
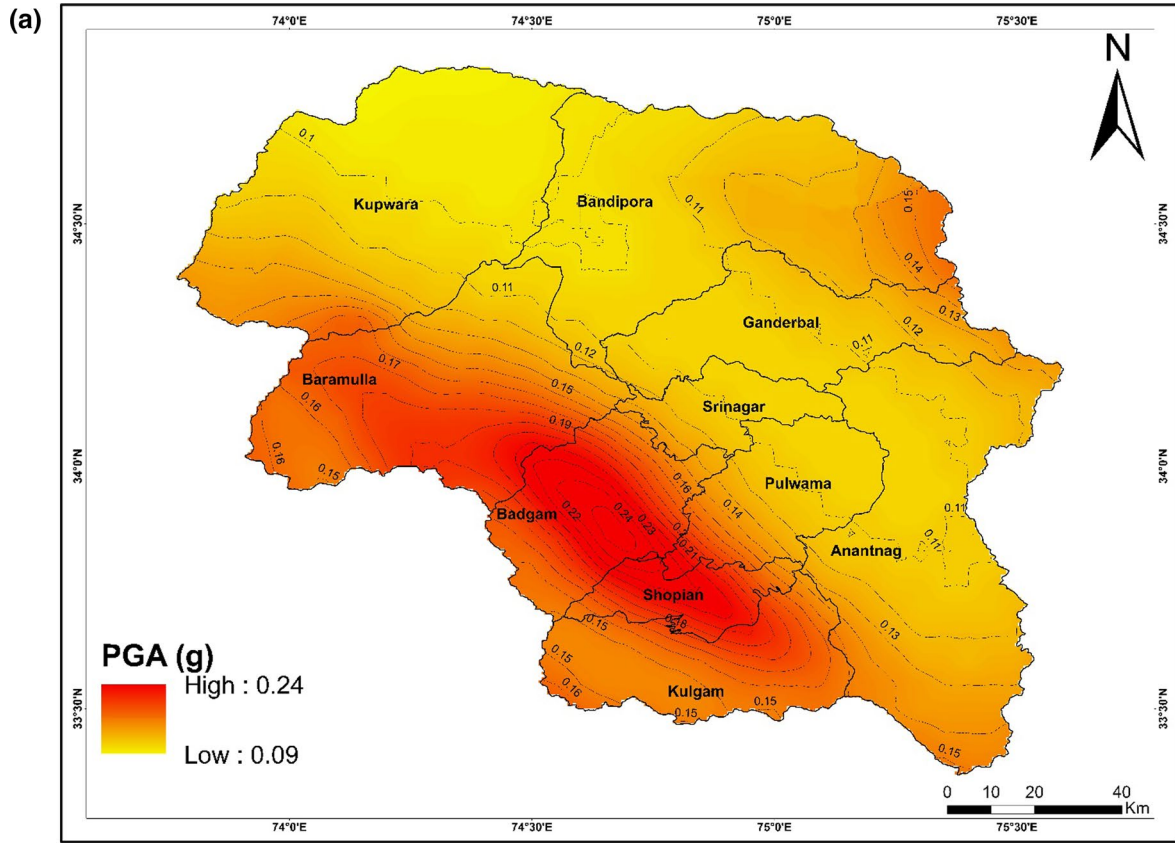


**Fig. 8** UHRS with 5% damping in some important cities (return period: **a** 50, **b** 100, **c** 500, **d** 2500 years)

imparting long-period resonance character to basin floor. On the other hand, the site effects play a crucial part in seismic hazard estimation. Drastic changes in PGA is observed when seismic waves travel from hard rock to Karewa deposits. Moreover, the effect of numerous proximate seismogenic source/faults is obvious in the hazard maps, which indicates locally high ground shaking close to seismic sources e.g. in and around Balapur and associated faults. Attenuation of seismic waves along strike shaking has also been observed during earthquakes in Himalayan region (Bilham 2019). Generally, by applying

**Fig. 9** **a** Hazard map for PGA corresponding 2 and 10% of probability of exceedance in 50 years with return period of 50 years. **b** Hazard map for PGA corresponding 2 and 10% of probability of exceedance in 50 years with return period of 100 years. **c** Hazard map for PGA corresponding 2 and 10% of probability of exceedance in 50 years with return period of 500 years. **d** Hazard map for PGA corresponding 2 and 10% of probability of exceedance in 50 years with return period of 2500 years

the combination of seismicity activity and paleoseismic data, the present hazard maps illustrate a more predictable ground motion scenario than pre-existing maps.





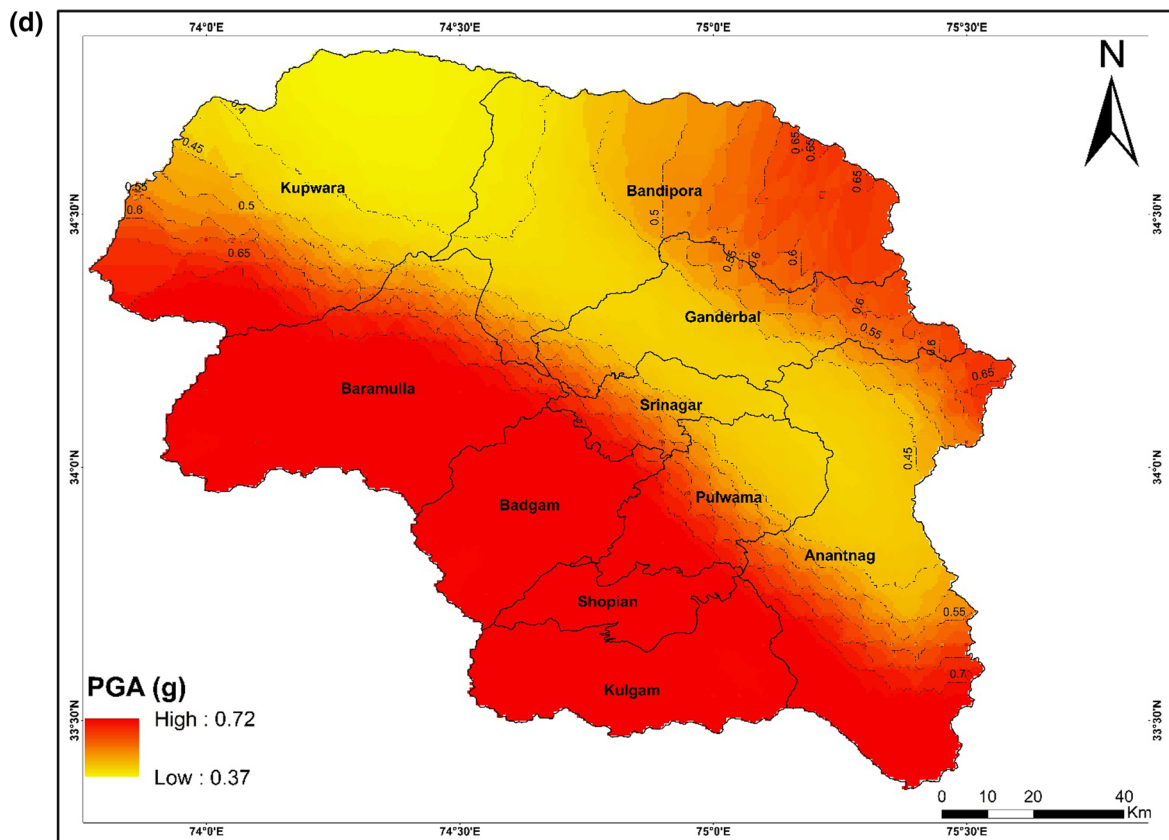
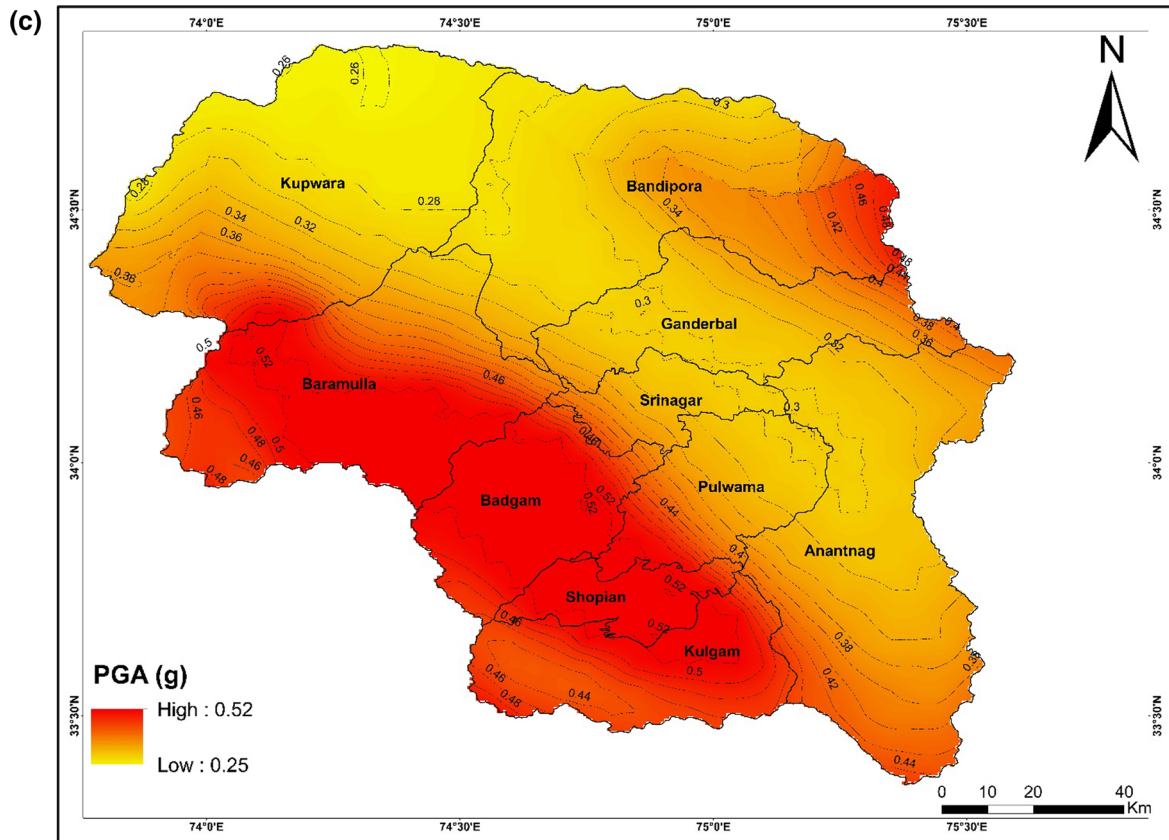
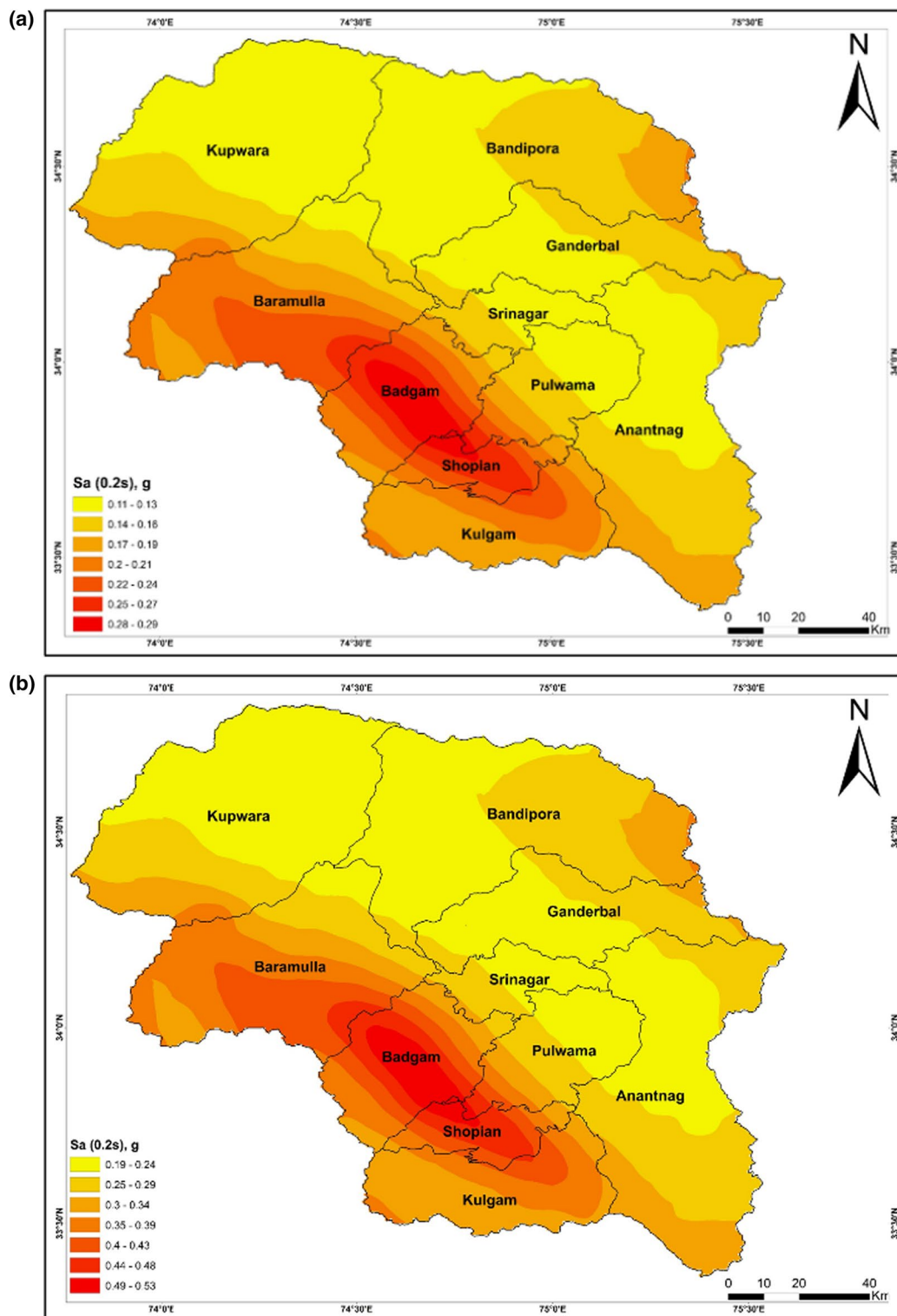


Fig. 9 (continued)





**Fig. 10 a** Hazard maps for spectral accelerations at 0.2 s structural period, corresponding to 2 and 10% probability of exceedance in 50 years with return period of 50 years. **b** Hazard maps for spectral accelerations at 0.2 s structural period, corresponding to 2 and 10% probability of exceedance in 50 years with return period of 100 years.

**c** Hazard maps for spectral accelerations at 0.2 s structural period, corresponding to 2 and 10% probability of exceedance in 50 years with return period of 500 years. **d** Hazard maps for spectral accelerations at 0.2 s structural period, corresponding to 2 and 10% probability of exceedance in 50 years with return period of 2500 years

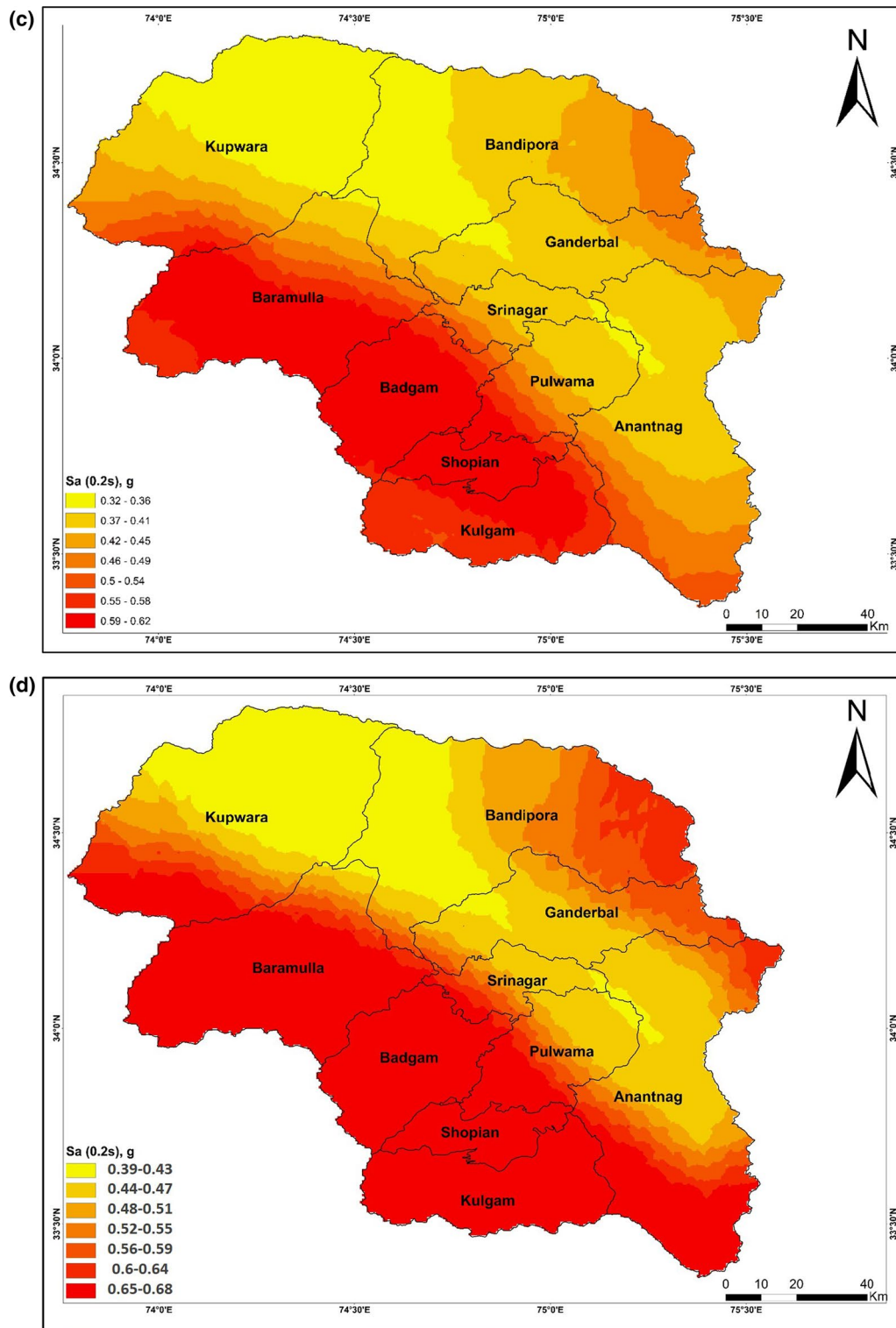
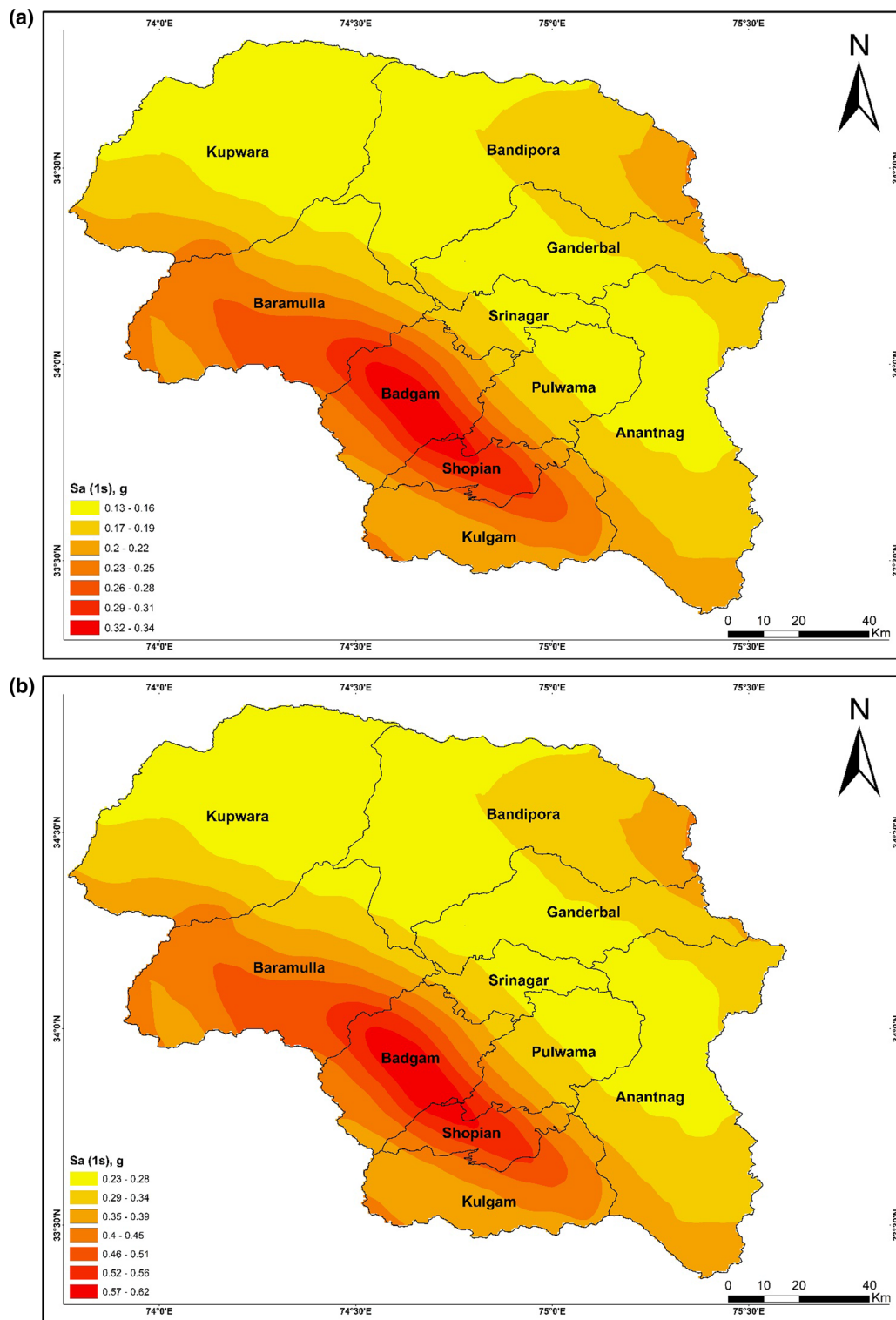


Fig. 10 (continued)



**Fig. 11 a** Hazard maps for spectral accelerations at 1 s structural period, corresponding to 2 and 10% probability of exceedance in 50 years with return period of 50 years. **b** Hazard maps for spectral accelerations at 1 s structural period, corresponding to 2 and 10% probability of exceedance in 50 years with return period of 100 years.

**c** Hazard maps for spectral accelerations at 1 s structural period, corresponding to 2 and 10% probability of exceedance in 50 years with return period of 500 years. **d** Hazard maps for spectral accelerations at 1 s structural period, corresponding to 2 and 10% probability of exceedance in 50 years with return period of 2500 years

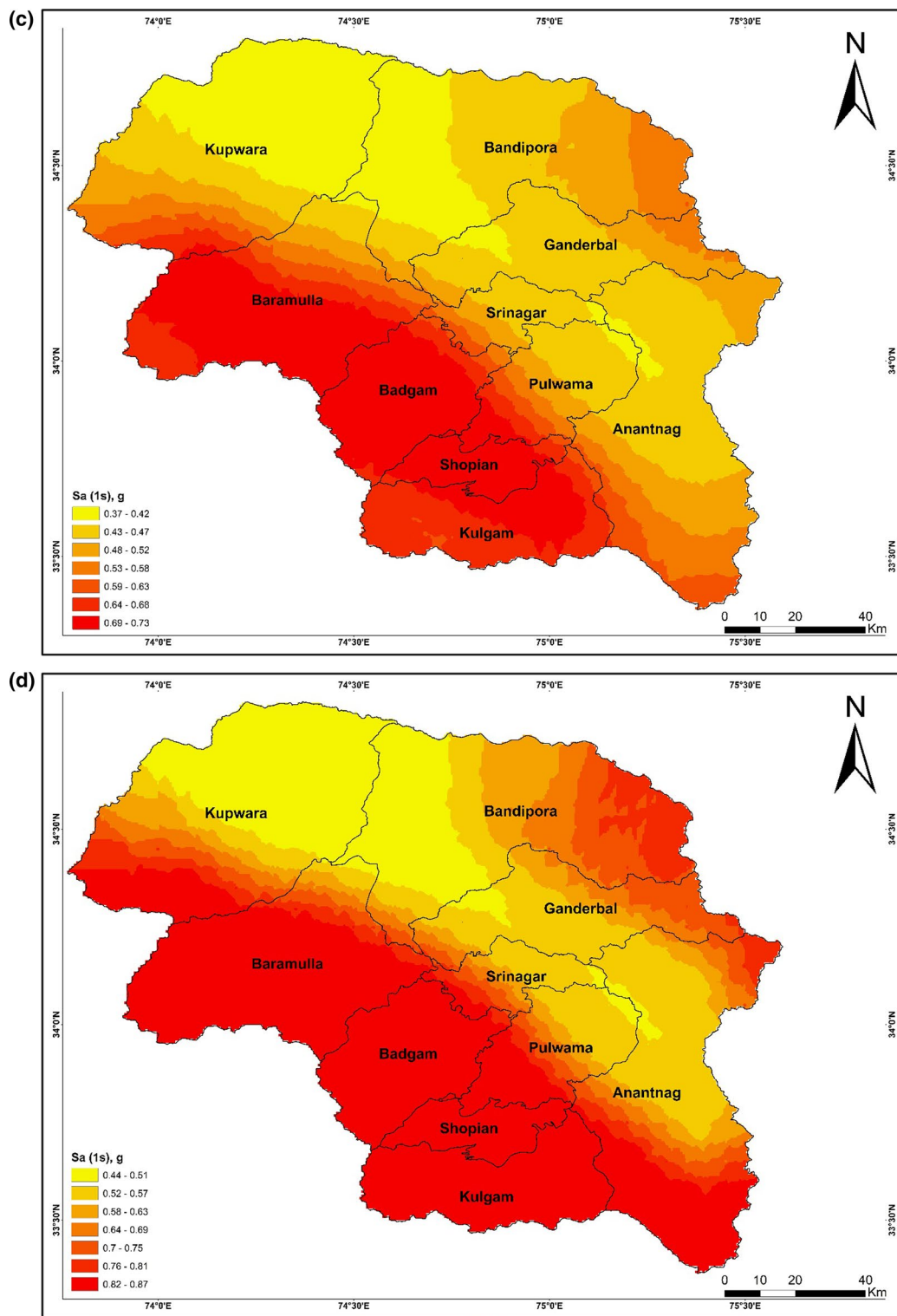


Fig. 11 (continued)



## Conclusion

The high population growth *visa viz* unplanned and unscientific construction techniques with high seismic vulnerability needs to be addressed vigorously to mitigate the level of seismic hazard imposed by future earthquakes. This study presents hazard maps for KB considering the regional geological setup, recurrent seismicity as well as local site conditions. Using the Cornell–McGuire approach the PSHA for KB has been estimated. An updated earthquake catalogue ranging from 25 to 2018 A.D. was used to designate the recurrence parameters for all 317 possible seismic sources/faults present within 500 km buffer zone of KB. We used empirical ground motion equations to estimate hazard curves for the all ten districts of KB for widespread NEHRP classes B and C (rock site) site conditions. We also obtained UHRS and HC from these seismic hazard maps four return periods (50, 100, 500, and 2500). Similarly, hazard maps as peak ground acceleration (PGA), short period ( $S_a$ , 0.2 s) and long period ( $S_a$ , 1.0 s) spectral acceleration, were estimated for the same return periods. On comparison with the previous studies, present study emphasizes local site conditions play important role in overall assessment and must be considered for site specific hazard evaluation. Our results show that areas neighbouring the districts of Shopian, Budgam, Kulgam and Pulwama possess highest hazard. The estimated values show that Indian codal provisions underestimate the level of hazard in this region. Therefore, results from present study prepared through broad framework are reliable and should be followed during design of new structures as well as seismic vulnerability estimation of the existing structures. Also, the estimated hazard maps along with UHRS and HC can be helpful to prepare risk maps of KB. The determined results suggest to robustly revise the existing construction/design guidelines of this region, and this study will be helpful for engineers, planners and designers to assess the probable future ground motions at the site and for risk evaluation.

## Compliance with ethical standards

**Conflict of interest** On behalf of all authors, the corresponding author states that there is no conflict of interest.

## References

- Abrahamson NA, Litehiser JJ (1989) Attenuation of vertical peak acceleration. *Bull Seismol Soc Am* 79(3):549–580
- Ahmad B, Shafi M (2014) Some more earthquakes from medieval Kashmir. *J Seismol* 18(3):681–686
- Ahmad B, Bhat MI, Bali BS (2009) Historical record of earthquakes in the Kashmir Valley. *Himal Geol* 30:75–84
- Ahmad B, Sana H, Alam A (2014) Macro seismic intensity assessment of 1885 Baramulla Earthquake of north-western Kashmir Himalaya, using the Environmental Seismic Intensity scale (ESI 2007). *Quat Int* 321:59–64
- Ahmad S, Alam A, Ahmad B, Bhat MI, Bhat MS (2015) Geomorphic evidence of unrecognized Balapur fault segment in the south-west Kashmir basin of northwest Himalayas. *Geomorphology* 250:159–172
- Algermissen ST, Perkins DM (1976) A probabilistic estimate of maximum acceleration in rock in the contiguous United States. US Geological Survey, Reston, VA, pp 76–416
- Ambraseys NN (2000) Reappraisal of North-Indian earthquakes at the turn of the 20th century. *Curr Sci* 79:101–114
- Ambraseys NN, Douglas J (2004) Magnitude calibration of north Indian earthquakes. *Geophys J Int* 159(1):165–206
- Ambraseys N, Jackson D (2003) A note on the early earthquakes in northern India and southern Tibet. *Curr Sci* 84(4):570–582
- Bhatia SC, Kumar RM, Gupta HK (1999) A probabilistic seismic hazard map of India and adjoining regions. *Ann Geophys* 42(6):1153–1164. 104401/ag-3777
- Bilham R (2004) Earthquakes in India and the Himalaya: tectonics geodesy and history. *Ann Geophys* 47:839–858
- Bilham R (2019) Himalayan earthquakes: a review of historical seismicity and early 21st century slip potential. In: Treloar PJ, Searle MP (eds) *Himalayan tectonics: a modern synthesis*, vol 483. Geological Society London Special Publications, London, pp 423–482
- Bilham R, Bali BS (2013) A ninth century earthquake-induced landslide and flood in the Kashmir Valley and earthquake damage to Kashmir's Medieval temples. *Bull Earthq Eng* 12:79–109
- Bilham R, Wallace K (2005) Future  $M_w > 8$  earthquakes in the Himalaya: implications from the 26 Dec 2004  $M_w = 9.0$  earthquake on India's eastern plate margin. *Geol Surv India Spec Publ* 85:1–14
- Bilham R, Gaur VK, Molnar P (2001) Himalayan seismic hazard. *Science* 293:1442–1444
- BIS, I. 1893 (2002, 2007) Criteria for earthquake resistant design of structures
- Boore DM (2009) Comparing stochastic point-source and finite-source ground-motion simulations: SMSIM and EXSIM. *Bull Seismol Soc Am* 99(6):3202–3216
- Bukhari SK, Maqbool Y, Dar AM (2018) A study of seismic resilience and construction techniques of Srinagar city Jammu and Kashmir India. *Disast Adv* 11(10):26–36
- Cárdenas M, Chávez-García FJ (2003) Regional path effects on seismic wave propagation in central Mexico. *Bull Seismol Soc Am* 93:973–985
- CENSUS (2001, 2011) Ministry of Home Affairs, Government of India
- Cornell CA (1968) Engineering seismic risk analysis. *Bull Seismol Soc Am* 58(5):1583–1606
- Dasgupta S, Pande P, Ganguly D, Iqbal Z, Sanyal K, Venkatraman NV, Dasgupta S, Sural B, Harendranath L, Mazumdar S (2000) Seismotectonic atlas of India and its environs. *Geol Surv of India Spec Publ* 59:1–43
- DeMets C, Gordon R, Argus DF, Stein S (1994) Effect of recent revisions to the geomagnetic reversal time scale on estimates of current plate motions. *Geophys Res Lett* 21:2191–2194
- Der Kiureghian A, Ang AHS (1977) A fault-rupture model for seismic risk analysis. *Bull Seismol Soc Am* 67(4):1173–1194
- Dunbar PK, Bilham R, Laituri MJ (2003) Earthquake loss estimation for India based on macroeconomic indicators CIRUS (Editor) Risk science and sustainability. Cooperative Institute for research in environment science. Boulder [https://doi.org/10.1007/978-94-010-0167-0\\_13](https://doi.org/10.1007/978-94-010-0167-0_13)

- Gardner JK, Knopoff L (1974) Is the sequence of earthquakes in southern California with aftershocks removed Poissonian? *Bull Seismol Soc Am* 64(5):1363–1367
- GSI (2000) Seismotectonic atlas of India and its environs geological survey of India, Bangalore, India
- International Code Council (ICC) (2009) International building code IBC 2009
- Iyengar RN, Ghosh S (2004) Microzonation of earthquake hazard in Greater Delhi area. *Curr Sci India* 87(9):1193–1202
- Iyengar RN, Sharma D, Siddiqui JM (1999) Earthquake history of India in medieval times. *Indian J Hist Sci* 34:3
- Joyner WB, Boore DM (1981) Peak horizontal acceleration and velocity from strong-motion records including records from the 1979 Imperial Valley, California, earthquake. *Bull Seismol Soc Am* 71(6):2011–2038
- Khattari KN, Rogers AM, Perkins DM, Algermissen ST (1984) A seismic hazard map of India and adjacent areas. *Tectonophysics* 108(1–2):93–134. [https://doi.org/10.1016/0040-1951\(84\)90156-2](https://doi.org/10.1016/0040-1951(84)90156-2)
- Kijko A (2004) Estimation of the maximum earthquake magnitude  $M_{max}$ . *Pure Appl Geophys* 161(8):1655–1681. <https://doi.org/10.1007/s00024-004-2531-4>
- Kijko A, Graham G (1998) Parametric-historic procedure for probabilistic seismic hazard analysis: part I: estimation of maximum regional magnitude  $M_{max}$ . *Pure Appl Geophys* 152(3):413–442
- Knopoff L, Kagan Y (1977) Analysis of the theory of extremes as applied to earthquake problems. *J Geophys Res* 82(36):5647–5657
- Kotha SR, Bindi D, Cotton F (2016) Partially non-ergodic region specific GMPE for Europe and Middle-East. *Bull Earthq Eng* 14(4):1245–1263
- Kotha SR, Bindi D, Cotton F (2017) From ergodic to region- and site-specific probabilistic seismic hazard assessment: method development and application at European and Middle Eastern sites. *Earthq Spectra* 33(4):1433–1453
- Kramer SL (1996) *Geotechnical earthquake engineering*. Pearson Education, London
- Kundu B, Yadav RK, Bali BS, Chowdhury S, Gahalaut VK (2014) Oblique convergence and slip partitioning in the NW Himalaya: implications from GPS measurements. *Tectonics* 33(10):2013–2024
- Madden C, Trench D, Meigs A, Ahmad S, Bhat MI, Yule JD (2010) Late quaternary shortening and earthquake chronology of an active fault in the Kashmir Basin. *Northwest Himal Seismol Res Lett* 81:346
- Madden C, Ahmad S, Meigs A (2011) Geomorphic and paleoseismic evidence for late Quaternary deformation in the southwest Kashmir Valley, India. Out-of-sequence thrusting, or deformation above a structural ramp? AGU Abstracts, T54B-07
- Mahajan AK, Thakur VC, Sharma ML, Chauhan M (2010) Probabilistic seismic hazard map of NW Himalaya and its adjoining area India. *Nat Hazards* 53(3):443–457
- Mandal P, Rastogi BK, Gupta HK (2000) Recent Indian earthquakes. *Curr Sci* 79:1334–1346
- McGuire RK (1976) FORTRAN computer program for seismic risk analysis. Open-file Report 76-67 US Geological Survey, Denver, USA
- Motazedian D, Atkinson GM (2005) Stochastic finite-fault modeling based on a dynamic corner frequency. *Bull Seismol Soc Am* 95(3):995–1010
- Muthuganeisan P, Raghukanth STG (2016) Site-specific probabilistic seismic hazard map of Himachal Pradesh India part II hazard estimation. *Acta Geophys* 64(4):853–884
- Nath SK, Thingbaijam KK (2012) Probabilistic seismic hazard assessment of India. *Seismol Res Lett* 83(1):135–149
- NDMA (2011) Development of probabilistic seismic hazard map of India. Technical Report of the Working Committee of Experts (WCE) National Disaster Management Authority (NDMA), Govt of India, New Delhi, India
- Parvez IA, Vaccari F, Panza GF (2003) A deterministic seismic hazard map of India and adjacent areas. *Geophys J Int* 155(2):489–508
- Peng KZ, Wu FT, Song L (1985) Attenuation characteristics of peak horizontal acceleration in northeast and southwest China. *Earthq Eng Struct Dyn* 13(3):337–350
- Quittmeyer RC, Jacob KH (1979) Historical and modern seismicity of Pakistan, Afghanistan, northwestern India and southwestern Iran. *Bull Seismol Soc Am* 69(3):773–823
- Raghukanth ST (2008) Ground motion estimation during the Kashmir earthquake of 8th October 2005. *Nat Hazards* 46(1):1–3
- Schiffman C, Bali BS, Szeliga W, Bilham R (2013) Seismic slip deficit in the Kashmir Himalaya from GPS observations. *Geophys Res Lett* 40(21):5642–5645
- Scordilis EM (2006) Empirical global relations converting  $M_S$  and  $m_b$  to moment magnitude. *J Seismol* 10(2):225–236
- Shah AA (2014) Comment on: “Macro seismic intensity assessment of 1885 Baramulla Earthquake of northwestern Kashmir Himalaya, using the Environmental Seismic Intensity scale (ESI 2007)” by Ahmad et al. 2013. *Quat Int*. <https://doi.org/10.1016/j.quaint.2014.04.064>
- Shah AA, Malik JN (2017) Four major unknown active faults identified, using satellite data, in India and Pakistan portions of NW Himalaya. *Nat Hazards* 88(3):1845–1865
- Sing SK, Ordaz M (1993) On the origin of long coda observed in the lake-bed strong-motion records of Mexico City. *Bull Seismol Soc Am* 83:1298–1306
- Stepp JC (1972) Analysis of completeness of the earthquake sample in the Puget sound area and its effect on statistical estimates of earthquake hazard. In: *Proceedings 1st international conference on Microzonation, Seattle, USA, vol 2, pp 897–909*
- Stidham C, Antolik M, Dreger D, Larsen S, Romanovicz B (1999) Three-dimensional structure influence on the strong motion wavefield of the 1989 Loma Prieta earthquake. *Bull Seismol Soc Am* 89:1184–1202
- Uhrhammer RA (1986) Characteristics of northern and central California seismicity. *Earthq Notes* 57(1):21
- USNRC (1997) USNRC Regulatory Guide 1165: identification and characterization of seismic sources and determination of safe shutdown earthquake ground motion. Unites States Nuclear Regulatory Commission Washington DC USA
- Wani AA, Bali BS, Lone S (2019) Drainage characteristics of tectonically active area: an example from Mawar Basin, Jammu and Kashmir, India. *J Geol Soc India* 93(3):313–320
- Wells DL, Coppersmith KJ (1994) New empirical relationships among magnitude rupture length rupture width rupture area and surface displacement. *Bull Seismol Soc Am* 84(4):974–1002
- Wyss M (2005) Human losses expected in Himalayan earthquakes. *Nat Hazards* 34:305–314
- Yousuf M, Bukhari KS (2019) Impact of geological and environmental complexities over infrastructure development in Kashmir Himalaya. *Disast Adv* 12(4):29–40
- Yousuf M, Bukhari SK (2020) Evaluation of seismically induced Soft Sediment deformation structures vis-a-vis their probable earthquake sources in Kashmir basin, NW Himalaya. *J Earthq Tsunami*. <https://doi.org/10.1142/S1793431121500032>
- Yousuf M, Bukhari SK, Dar AM, Mir AA (2018) Seismic Vulnerability Assessment of major construction pattern of the of Srinagar city. *Int J Recent Trends Sci Eng* 7(4):1889–1901
- Yousuf M, Bukhari SK, Bhat GR, Ali A (2020) Understanding and managing earthquake hazard visa viz disaster mitigation strategies in Kashmir valley, NW Himalaya. *Prog Disast Sci* 5:100064